THE EFFECT OF INFUSING TiO_2 NANOPARTICLES ON THE OPTOELECTRONIC PROPERTIES OF MEHPPV THIN FILMS FOR OLED FABRICATION.

A Thesis Submitted to the Department of Materials Science and Engineering

African University of Science and Technology

In Partial Fulfilment of the Requirements for the Degree of

MASTER OF SCIENCE in Materials Science and Engineering

BY

NALYANYA FRED

Abuja-Nigeria

SUPERVISOR**: Dr. Vitalis Chioh Anye**

September, 2021

CERTIFICATION

This is to certify that the thesis titled "The Effect of infusing TiO_2 Nanoparticles on the optoelectronic properties of MEHPPV Thin Films for OLED Fabrication**.**" submitted to the school of postgraduate studies, African University of Science and Technology (AUST), Abuja, Nigeria for the award of the Master's degree is a record of original research carried out by NALYANYA FRED in the Department of Materials Science and Engineering.

THE EFFECT OF INFUSING TIO2 NANOPARTICLES ON THE OPTOELECTRONIC PROPERTIES OF MEHPPV THIN FILMS FOR OLED FABRICATION.

By
NALYANYA FRED

A THESIS APPROVED BY THE DEPARTMENT OF MATERIALS SCIENCE AND ENGINEERING

RECOMMENDED:

_____

Supervisor: Dr. Vitalis Chioh Anye

_____

Prof. Peter Azikiwe Onwualu
Head, Department of Materials Science and Technology

APPROVED: _____

Chief Academic Officer

_____

Date

ABSTRACT

The use of MEHPPV in OLED application has increased currently. The main issue surrounds its ability to perform well optically and electronically. To enhance the performance of MEHPPV polymer in this sense, this study looks at infusing TiO2 nanoparticles at different percentages from 0.1g TiO2 in MEHPPV polymer to 0.5g TiO2 in MEHPPV polymer in increasing ranges of 0.1g and examining the performance. Several techniques such as UV-Vis, SEM, and XRD were used. The future looks at the possible use of the four-point probes and nanoindentation in checking the performance in addition to the techniques used to establish a greater information base. The solution of the combination of these two chemicals will be spin-coated onto two types of glasses to form a thin film for examination using the mentioned techniques above. This will be done while varying the composition of TiO_2 up to an optimum level, that improves performance but does not compromise mechanical properties.

Keywords: Solar-Cell, MEHPPV, TiO_2, OLEDs, Structure, Morphology, FTO, Bare glass, UV-Vis.

ACKNOWLEDGEMENT

I give all thanks and praises to God Almighty for life, health, wisdom, strength, provision and divine favor He blessed me with, to enable me carryout my master's program and thesis successfully. I am who I am today by His Grace, Love and Mercy.

My sincere appreciation fully goes to my all family members, relatives and friends for their endless supporting hand they have always extended to me, just to see me achieve such great levels. My father, Walwema Vincent and my mother Kalibo Janet, take the largest portion as they have been light and the source of provision always and everywhere.

My heartfelt gratitude goes to my supervisor Prof. Vitalis Anye for his devoted guidance, time, patience, encouragement and support which led to the success of this research. He believed in me and my ability to carry out any responsibility and shows continuous interest in my career. His interest and enthusiasm for science and renewable energy was a source of inspiration. He fully dedicates his time to drive me towards my goals. I extend my appreciation to our dear Head of Department, Material science and Engineering, Prof. Azikiwe Peter Onwualu for his parental care and distinguished leadership. He deep heartedly considers the concerns of all the people he leads and attends to all with satisfaction.

Huge thanks to Prof Wole Soboyejo for his early nurturing and pure introduction to the concepts of this field and Prof. Douglas J. Buttery for his academic support. I thank the entire material science and engineering department instructions team for grooming us intellectually, with gladness, including my colleagues. I can hardly forget the post masters students and the PhD students of the time like Chukwudalu Claire, Theresa, Dr Kigozi Moses, Numfor Bih and Henry among others for their tireless support of my entire course. May God bless you all.

TABLE OF CONTENTS

LIST OF FIGURES

1 CHAPTER ONE: INTRODUCTION

1.1 Background

In the recent past, in attempts to ensure a better and affordable process of solar cell, more people have diverted their attention towards Dye Sensitized Solar Cell (DSSC) (S. Kumar et al., 2018; Lira-cantu & Krebs, 2006) This is because of the inexpensive fabrication process, lightweight which is very suitable for autonomous sensors, easy to dispose and are environmentally sound (Norhisamudin et al., 2020).

DSSC also has extremely high optical absorption coefficients and the single layer of DSSC is the simplest form (Al-asbahi, 2018). It contains a layer of organic electronic material that is in between two metallic conductors which works as anode and cathode (Mosharraf Hossain Bhuiyan et al., 2021). The different function of the metallic conductor will set up a flow of current in the organic layer (Hou et al., 2019). The dye that is used in the DSSC absorbs the light and form a photon to travel through the metallic conductors to form a photocurrent (Roy et al., 2020).

TiO_2 is a nanoparticle that has three different phases which are rutile, anatase and brookite (S. H. Yang et al., 2007). In order to have the most thermodynamically stable phase, rutile structure has the most suitable phase for it while the other two are metastable (N. S. Kumar & Babu, 2021). However, for this experiment, we used the anatase phase because it has wider energy band gap, which is 3.2 eV and suitable for the photon scattering process in the DSSC.

In this project, compositions of TiO_2 in MEHPPV were varied with hope of improving surface morphology and optoelectronic properties.

The photoanode surface coated with TiO_2 tends to crack easily and does not give enough mesoporous surface in order to absorb dye (Chergui et al., 2011). Hence, for improvement of the mesoporous surface, the photoanode is developed by doping of Poly(2-methoxy-5-(2'-ethylhexyloxy)-1,4-phenylene-vinylene (MEH-PPV) and Titanium Dioxide (TiO2) layer on Indium Tin Oxide (ITO) glass which is immersed in the dye solution (Al-asbahi, 2021). In this particular experiment, we used Florine-doped tin oxide (FTO), glass instead of ITO due to its availability. Bare glass was also used and compared with the FTO type MEH-PPV is commonly

used in the fabrication of the Organic Light Emitting Diode (OLED), and this research work this time entirely focuses on improving its performance for OLED applications (Al-asbahi, 2018; Hieu, 2012) When high temperature is applied on the polymer, it evaporates and leaves holes on the TiO_2 surface hence leading to the increasing of surface roughness (Dinh et al., 2009; S. H. Yang et al., 2007).

However, there are several risks that might occur in the process. In order to get a high efficiency, the photoanode layer needs to have a very high porosity surface. This can make the dye to be absorbed much easier.

This is because when the absorption of dye increases, the number of photons will be increased and produces a greater performance of DSSC (A Petrella et al., 2004). This makes the reasoning to find an optimum ratio between TiO2: MEH-PPV concentration as the main point for this study. MEH-PPV is used as medium to increase the amount of porous in TiO2 (Ibrahim & Sharhan, 2019). However, this study has not looked at which suitable temperature. This is because temperature was not opted for as a variable (this will be investigated during the future studies). Main processes that are involved in this solar cell include the absorption of the photon by the MEH-PPV in order to generate a photon and the photon will move toward the donor or the acceptor. Therefore, many photons can be generated with the presence of the MEH-PPV.

Few decades down the road, statistics has shown that conjugated aromatic polymers have attracted considerable interest because of their diverse applications, ranging from electronic devices to light emitting diodes and photovoltaic devices (Dinh Van, 2015). Although these polymers exhibit moderate photoluminescence (PL) quantum efficiencies and their application in light-emitting diode devices is hampered by the formation of chain aggregates in the solid state. Many studies have attempted to enhance the quantum efficiency by regulating the conjugation length, blending with small organic molecules, changing the polymer structures to form asymmetric poly (this p-phenylene vinylene) derivatives, or using an electron-transporting layer. The major approaches to improve the luminescent efficiency of polymers are attaching bulky side groups to the main-chain structures to alter the polymer inter-chain distance. In recent years, greater interest has been directed toward the study of hybrid organic/inorganic nanostructures, owing to the possibility of combining the electrical properties of semiconducting organic

polymers with the optical peculiarities of inorganic nanostructures like rods, particles, and thin films. The energy transport and electron transport properties of these conjugated polymer/inorganic nano-crystals and nanocomposites have been explored in several studies (Victoria et al., 2021a). TiO_2 nanocrystals blended with electroluminescent organics have shown lasing action with greatly reduced threshold pump powers (Al-asbahi et al., 2019). Previous studies concerning TiO_2/MEH-PPV composites films indicated that their electroluminescence (EL) increases with the size of the TiO_2 nanoparticles, the crystal structure of TiO_2 also plays an important role (A Petrella et al., 2004; Victoria et al., 2021b). This is one of the reasons for increasing EL efficiency in the TiO_2 particles/MEH-PPV studies (Norhisamudin et al., 2020; Zahid et al., 2012)

In the recent study, Anatase-TiO_2 mixing with MEH-PPV at volume rate (0.01:0.002 and 0.01:0.008) mg/ml for MEH-PPV/TiO_2 was done in which they proposed a new approach which blends needlelike TiO_2 nanostructures into MEH-PPV polymer in order to form percolation network geometry (A. De Caro, 2015; Al-asbahi et al., 2019). They investigated the effect of the addition of these TiO_2 nanoparticles on the electrical properties by I-V measurement and the spectrum of EL. This closely relates to my experiment only that in this case, morphology and optoelectronic properties are to be analyzed by Scanning Electron Microscopy (SEM) and UV-Vis techniques respectively. Mechanical properties of the generated films were to be investigated but the necessary instrument (Nanoindenter) had a technical problem and so such results were not obtained.

1.2 Problem Statement

The MEHPPV thin films application in OLEDs are found to have low and limited charge carrier injection capability, low stability and low electron transition probability due to poor uniformity and porosity of the surface morphology. This hinders the electron transport and leads to short lived devices in general and so OLEDs application of MEHPPV is limited as a result. For proper and enhanced performance, we need a better charge carrier infection, improved stability and reduced conjugation length that will give an overall positive influence on the MEHPPV for OLEDs applications. This is expected to be improved through variation of Anatase TiO2 composition in MEH-PPV and observing the changes brought by such changes.

1.3 Objectives

1.3.1 General objective

To study and optimize the optoelelctronic properties of the MEHPPV active layer for Organic Light Emitting Device applications by reducing the contact length and improving electron collection to achieve higher power conversion efficiency.

1.3.2 Specific objectives

i. To fabricate thin films: the control film (only MEHPPV without infusing any nanoparticles), other sets of films with TiO2 nanoparticles infused in MEHPPV with varying compositions. This will be by spin coating using a two-step process on an FTO coated glass substrate at room temperature.
ii. To study the effect of varying composition of TiO_2 on the optical and electrical properties on MEHPPV polymer. The properties will be checked by use of UV-Vis, SEM, among other techniques.
iii. To analyze the morphological variations with varying TiO2.

.

1.4 Outline of the Thesis

Chapter one gives a general introduction of the current energy need, solar power and its technologies. It also includes the aim and objectives of this research work.

Chapter two is a literature review on the world's energy need, energy challenge of Africa and how the economy is being affected. It also gives a review on the fundamentals of photovoltaic and evolution of solar cells.

Chapter three presents the experimentation steps carried out in this research.

Chapter four covers the description of the experimental procedure for the work being carried out. The results obtained and discussion of the results is presented in chapter five. Conclusion and recommendations for future work were presented in chapter six.

2 CHAPTER TWO: LITERATURE REVIEW

2.1 MEHPPV Thin Films and Titanium Dioxide (TiO_2)

2.1.1 General description

MEH-PPV is a conducting organic semiconductor which has low molecular weight and hydrophobic characteristics. It is a poly(phenylenevinylene) (PPV) derivative and a conjugating polymer with highest occupied molecular orbital (HOMO) below the fermi level of gold. It is a Light-emitting conjugated polymer. Titanium Dioxide (TiO2) is one of the main materials in Dye Sensitized Solar Cell (DSSC). It is well known with its property of good optical transmittance and its mesoporous surface that can absorb generous amount of dye. In this study, TiO2 and MEH-PPV films are fabricated using spin coating technique that leads to the uniform thickness of TiO2 and MEH-PPV layers (Lira-cantu & Krebs, 2006; Tripathi et al., 2006).

2.1.2 Application

Organic Semiconductor Laser Materials, Conducting polymer in solar cells and carbon nanotube OLEDs. It is useful in producing bright and efficient white polymeric light emitting diodes. Filter before application. MEH-PPV can form a nanocomposite with carbon nanotubes (CNTs) by spin coating that can be used for H_2S gas sensors. It can also be used as a conducting polymer which results in the formation of a low-cost dopant free hole transporting material (HTM) for the fabrication of Perovskite solar cells with a power efficiency of 9.65%. MEH-PPV can be blended with PCPDTBT for use as a sensitizer for dye sensitized photo sensors (DSPS).

2.1.3 Packaging

i) 1 g in glass bottle
ii) 250 mg in glass insert

2.1.4 Safety Information

a) Personal Protective Equipment
b) Eyeshields, Gloves, type N95 (US)

2.1.5 History and Previous Studies on MEHPPV thin films

MEHPPV as a material has been identified as active layers for OLED applications. Conjugated polymers are nowadays used in several display applications, resulted from intensive research works over the last decade since the first report on polymer-based light emitting diodes. Among them, poly (*p*-phenylene vinylene) (PPV) and its derivatives have attracted a great deal of attention because of their particular structure and their highly interesting electroluminescent properties (Andrea Petrella et al., 2005).

To enhance the performance of PPV-based devices, several studies have been carried out on composites made with polymers and nano-oxide particles such as silicon oxide (SiO2) or titanium oxide (TiO2). The former is found to have a good effect on the conductivity of the polymer host while the second can influence its photovoltaic properties (Tripathi et al., 2006). The use of composites is believed to increase the electrical conduction of the polymer and in addition, to improve its stability, which is of prime importance in organic devices (S. H. Yang et al., 2007). When used in composites, modifications of the polymer luminescence were observed for both oxides. However, contradictory results have been reported. For example, poly(2-methoxy-5-(2'-ethylhexoxy) -1,4-phenylene vinylene) (MEH-PPV) blended with SiO_2 was found to have an improved conductivity as compared to the bare polymer, while PPV with similar nanoparticles shows a lower conductivity than the polymer alone (Lira-cantu & Krebs, 2006).

Besides, the effects of the nanoparticles on the structure of the polymer are still a subject of research.

Baraton *et al.* found that blends using TiO_2 nanoparticles do not break the PPV conjugation and possess the potential of gas sensing applications. Zhang *et al.* observed that the TiO_2 nanoaggregates take the form of a sphere and change into an ellipsoid as the content of TiO_2 increased. From our previous report, SiO_2 nanoparticles would reduce the conjugation lengths of PPV and the reduction becomes significantly important as the content of SiO_2 increases [13]. Comparing samples having different nanoparticle sizes and a similar oxide concentration, we found that smaller nanoparticles induce larger blue shift (Nanoparticles et al., 2020).

The previous mentioned composites use PPV as a polymer host matrix (Sarah et al., 2011). For this material, a thermal conversion process is required to obtain the final conjugated polymer. In this work, we have studied composites made by incorporation of SiO2 or TiO2 nanoparticles of different concentrations and sizes in MEH-PPV. Since MEH-PPV is a soluble conjugated polymer, one can incorporate oxide nanoparticles into MEH-PPV directly. We examine the optical properties of the hybrid materials and discuss the influence of the nature and the size of the particles on the behavior of the composites.

In this work, we shall investigate the optical properties of MEH-PPV and its nanocomposites made by incorporating TiO_2 nanoparticles into polymer layer at varying compositions. Previous studies have shown that the conjugation length of the polymer is not affected by the presence of the particles, whatever their concentration (up to 8%) and their nature, in contrast to results obtained in PPV/oxide nanocomposites. It shows furthermore that the studied composites present a higher stability in emission characteristics compared to bare polymer films. This stability is explained as a consequence of the reduction of the formation of carbonyl type groups in MEH-PPV, resulted from the presence of the nanoparticles. It is probable that the conservation of the conjugation length plays an important role in the stability of the polymer but it is also obvious that the particles limit or even reduce the formation and diffusion of oxygen inside the polymer matrix. The high stability of the composites makes them attractive for fabrication of photoactive devices, especially for TiO_2 based composites, which can be used in polymer photovoltaic cells.

The thickness of the TiO_2 can be controlled layer by layer using same technique to get an optimized surface that can lead to better performance of DSSC. In order to achieve this, the surface roughness of TiO_2 must be as high as possible.

Therefore, the organic material which is Poly(2-methoxy-5-(2'-ethylhexyloxy)-1,4-phenylene-vinylene (MEH-PPV) is used as medium to increase the mesoporous roughness structure of TiO_2 nanocrystal film for DSSC. MEH-PPV is doped into the TiO2 using 0.5 mg/ml with different temperatures of 100^0C and 450^0C. Different temperatures of MEHPPV will lead to the different surface structures for TiO_2 thin film. The ratios of TiO2: MEH-PPV used were 1:1 and 2:1. The surface of TiO_2 thin film was characterized using Atomic Force Microscope (AFM). The efficiency was obtained using Solar Simulator based on the voltage and current flow. Based on

the results, the increment of surface roughness is about 21% for the different ratio at various temperatures. The optimum temperature and suitable ratio of TiO_2: MEH-PPV was obtained via annealing process at 450^0C with the ratio of 2:1. It gives the highest efficiency which is 0.1266%. These two important findings yield good mesoporous surface of TiO_2 thin film.

2.1.6 TiO_2 when infused in polymers; MEH-PPV and PCB

In addition, more related research works have gotten MEH-PPV, [6,6]-phenyl-C61-butyric acid methyl ester (PCBM) and inorganic semiconductor nanoparticles (n-TiO2) dissolved, mixed and spin-coated them on indium tin-oxide (ITO) substrate. The incorporation of the n-TiO2 nanoparticles changes the morphology and increases the roughness of polymers film (MEH-PPV/PCBM). Characterization by cyclic voltammetry showed the electrochemical stability of the composite material, and the photocurrent density characteristic of the composite (MEH-PPV/PCBM+n-TiO2) was higher than that of the single MEHPPV/PCBM film. The study showed that the presence of n-TiO2 particles in the polymeric film improves the photoelectrochemical properties of MEH-PPV/PCBM and gives information on the possibility of application in organic-inorganic photovoltaic cells.

2.2 Organic Light Emitting Diode (OLED)

The I-V characteristics of MEH-PPV and MEH-PPV/(Anatase)TiO2 nanocomposite preparing by multi layers using ITO (anode)/PEDOT: PSS(HTL)/MEH-PPV: TiO2 (EL)/ALq3 (ETL)/AL (cathode) were deposited using spin coater, also assuming the formation of HTL as PEDOT: PSS and ETL as Alq3 during anode and cathode electrode, lowering the barrier or creating a tunneling path for majority and minority carrier (Ibrahim & Sharhan, 2019). The current–applied voltage curves of nanocomposites with different weight ratios of Titania nanoparticle. As the weight ratio of nanoparticles increases, the device current increases. The p-type conductive property of Titania nanoparticles can improve the hole-transporting ability of the MEH-PPV layer (Al-asbahi, 2018). Significantly lower injection barriers are achieved in the nanocomposites because of the reduction barrier for the injection of holes from the ITO anode to the Titania nanoparticles (Dinh et al., 2009). Also, as a result of doping with Titania nanoparticles the onset voltages decreased from (1 to 0.5) V up to (0.002) g/ml. For higher

doping ratios of Titania nanoparticles, no changes in the onset voltages are observed (Al-asbahi, 2021).

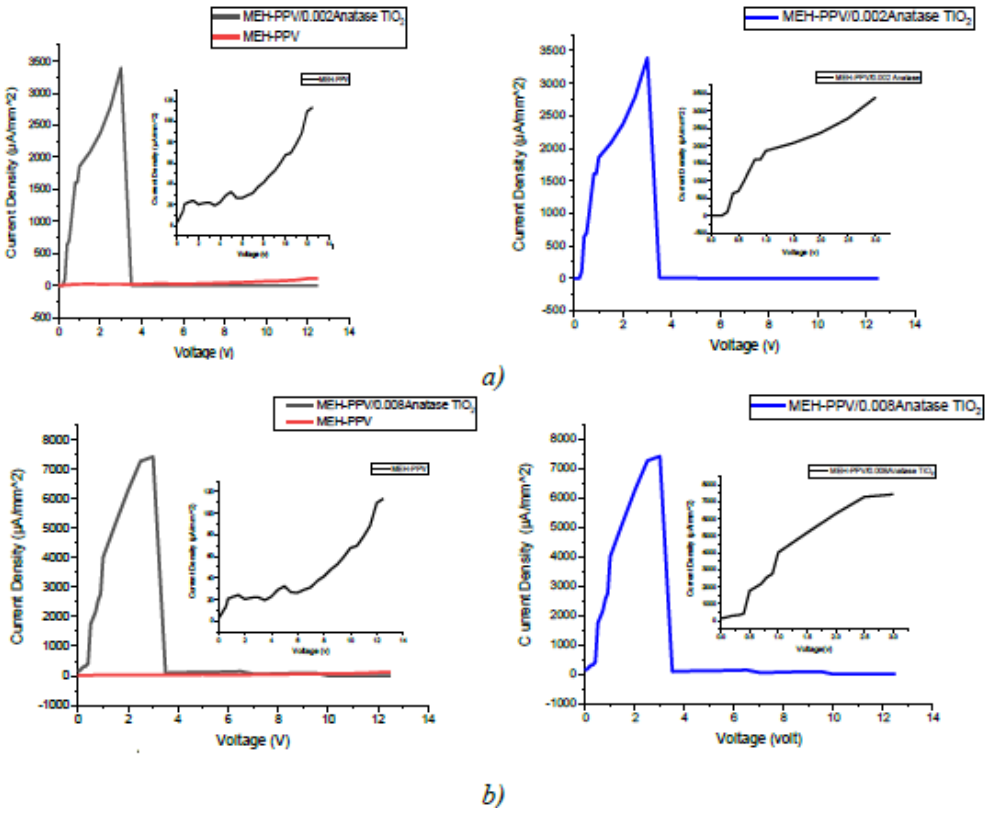

Figure 2.1: (a) J-V characterize of pure organic polymer MEH-PPV and mixing with (0.002) TiO2, (b) J-V characterize of MEH-PPV and mixing with (0.008) TiO2

2.2.1 The Drive for MEHPPV and Possible Element Infusions for OLEDS.

Polymer and organic light-emitting diodes (OLEDs), photovoltaic cells and field effect transistor are being focused towards commercialization. Poly[2-methoxy-5-(2'-ethyl-hexyloxy)-1,4-phenylene vinylene] or known as MEH-PPV, have been extensively studied for OLED applications. Related studies have had MEH-PPV powders dissolved in toluene and 1, 2-dichlorobenzene (1, 2-DCB) at different solutions concentration and deposited using spin coating technique. In most cases, surface morphologies of the films are obtained using Atom Force Microscope (AFM) and thickness using surface profiler, while the electrical properties are investigated using 2-point probe. The optical properties are characterized using UV-Visible-NIR

(UV-VIS-NIR), and photoluminescence (PL) spectrometer. The surface roughness, Ra of the films has been noted to increase with the concentration for both types of solvent, however for films in toluene, as the concentration increases well above 5mlmg -1, the roughness decreases which is caused by the aggregation of the MEH-PPV. Films' thicknesses increase as well as the resistivity for both types of solvents. However, for MEH-PPV thin films in 1, 2-DCB show better conductivity compared to toluene. PL spectra of films using toluene are red-shifted due to longer conjugation length, and also show higher intensity compared to films using 1,2 DCB.

2.3 Perovskite Solar Cells (PSCs)

2.3.1 Electron transport materials (ETMs)

The ETM transports electrons injected from the absorber layer (perovskite) to the electrode where they are collected. A number of in organic metal oxides, such as TiO_2, ZnO, SnO_2, SiO_2, ZrO_2, can either be used as ETM or scaffold material (Moore & Wei, 2021). The most important characteristic of an ETM is that it must satisfy band alignment with the perovskite layer, i.e., it should have lowest unoccupied molecular orbital (LUMO) and highest occupied molecular orbital (HOMO) higher than the perovskite active layer (Oyelade et al., 2020). It must have high transmittance in the UV-Vis region so that a photon can pass through easily and be absorbed by the perovskite absorber (Mahmood et al., 2017).

The most commonly used ETM for mesoporous perovskite solar cells is TiO_2, although oxygen vacancies and titanium interstitials can form in this layer. These defects cause deep sub-band gap trap states, which reduces solar cell performance (Roy et al., 2020). Oxygen is required to passivate these traps; however, other layers in the device requires encapsulation to prevent moisture entry which degrades the solar cell (Liu et al., 2016).

2.3.2 Film Deposition Methods

Many approaches have been reported for the synthesis of perovskite active layers which are; one-step precursor solution deposition, two- step sequential deposition, dual-source vapor deposition, vapor assisted solution process and sequential vapor deposition.

2.3.2.1 One-step spin-coating method

One-step solution processing is the simplest of the solution processing technique for the growth of perovskite, this method involves the spin coating of a precursor solution of lead halide with a certain amount of an organic ammonium halide (Ahmed et al., 2015), Spin coating deposits uniform thin films on flat substrate which rotates at a high speed (> 600 rpm). The perovskite crystallites form and grow during the solvent evaporation. A post-annealing process is carried out at a relatively high temperature (around 100 °C) for the complete crystallization of the perovskite and the removal of the residual solvents. The annealing temperature, solution concentration, precursor composition and solvent choice influences the film morphology and PSCs performance (Zheng et al., 2015). Gamma-butyrolactone (GBL), dimethylformamide (DMF), and dimethyl sulfoxide (DMSO) are examples solvents that are being used for the dissolution of the precursors. Mixture of solvents (DMF and GBL, DMF and DMSO, DMSO and GBL) have also been reported for obtaining optimum concentrations for solution processing since higher concentrations lead to better film coverage and higher efficiency devices owing to the rapid evaporation of this combination of solvents (Ahmed et al., 2015). Im et al, reported the one-step coating method for iodide perovskite active layer by reacting equimolar CH_3NH_2 and HI in the appropriate solvent. The synthesized CH_3NH_3I was then mixed with PbI_2 at a 1 : 1 molar ratio in GBL at 60^oC then the solution is put under stirring for several hours after which it is used as a coating solution.

2.3.2.2 Two-step spin-coating method

In a two-step deposition processes, the lead salt is dissolved in DMF and deposited on the substrate, when the lead iodide film is dried on hot plate for a short time like 10 minutes, a solution of methyl ammonium iodide (MAI) dissolved in isopropyl alcohol (IPA) is used to convert the lead iodide film into perovskite (Bastiani, 2016; L. Yang et al., 2016). This step can be realized in very different ways: dipping the lead film into the MAI solution, spin-coating the solution MAI on top of the lead film or exposing the lead film to MAI vapours after which the perovskite film is annealed (Bastiani, 2016).

2.4 UV-VIS

Many chemical compounds have a characteristic color. For example, quinone is yellow; chlorophyll is green; the 2, 4-dinitrophenylhydrazone derivatives of aldehydes and ketones range in color from bright yellow to deep red, depending on double bond conjugation; and aspirin is colorless. All these colors are caused by absorption of light in the visible region of the electromagnetic spectrum (400 - 800 nm under excitation of an electron from the ground state into a higher orbital. In this experiment you will become familiar with the handling of a commercial spectrometer and use absorption spectra to determine the pK_a value of an indicator (Nanoparticles et al., 2020).

2.4.1 Absorption of Radiation

Electronic orbitals of atoms and molecules have characteristic energies, giving rise to a set of discrete energy levels. An electron is able to change from an occupied orbital to another orbital, gaining or losing energy only in amounts exactly corresponding to the difference between two levels: The transition from the ground state (lowest possible energy) at energy E_0 to a higher level at energy E_n is possible if the molecule absorbs electromagnetic radiation of the corresponding wavelength $\lambda = ch/(E_n - E_0)$, where c is the speed of light and h is Planck's constant. Excited states usually exist only for a very short period of time (femtoseconds to microseconds), because the higher energy state is unstable and the extra energy is lost through relaxation processes such as emission of light (see the Experiment Fluorescence Quenching). The typical energy difference between the ground and the first excited levels of many molecules corresponds to electromagnetic waves of the ultra-violet (UV) and visible regions of the electromagnetic spectrum (Han et al., 2021).

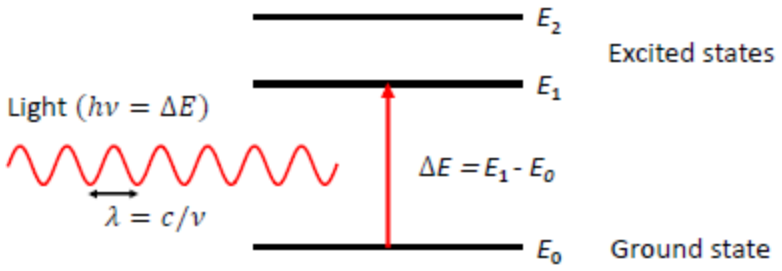

Figure 2.2: Different Energy levels.

2.4.2 The Electromagnetic Spectrum

The UV-visible range is only a small part of the total electromagnetic spectrum, and is generally defined from wavelengths of 190 nm at the high energy UV end to about 750 nm at the low energy red end of the spectrum. Light in other regions of the spectrum gives rise to different types of transitions and is the subject of different types of spectroscopy. For example, IR radiation is usually not energetic enough to cause electronic transitions but can excite vibrations of molecules. The wavelength ⅄ is the distance between adjacent peaks (or troughs) in the time-frozen electromagnetic wave, and is given in meters, centimeters or nanometers (10^{-9} meters).

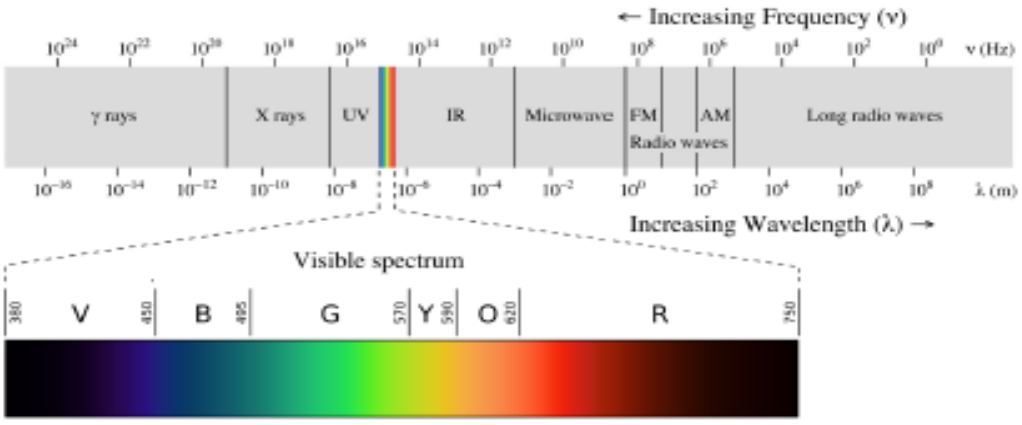

Figure 2.3: The Electromagnetic Spectrum

Visible wavelengths cover a range from approximately 400 to 750 nm. The frequency *v* is the number of wave cycles that travel past a fixed point per unit of time, and is usually given in cycles per second, or Hertz (Hz). Frequency and wavelength are related via

$$\lambda = c/\nu = \frac{2\pi c}{\omega}$$

where c is the speed of light. The angular frequency $\omega = 2\pi\nu$ (radians per second) is often used instead of ν. When polychromatic or 'white' light passes through or is reflected by a colored substance, a characteristic portion of the spectrum is absorbed. The remaining light will then exhibit the complementary color to the wavelength(s) absorbed. Thus, absorption of blue light between 420-430 nm renders a substance yellow, and absorption of green, 500-520 nm light makes it red. Green, to which our eyes are most sensitive, is unique in that it can be created by absorption close to 400 nm as well as absorption near 800 nm.

2.4.3 Absorbance and Electronic Transitions

2.4.3.1 The Lambert-Beer Law

After crossing a thin slice Δx of absorbing sample, the light intensity I(Δx) is smaller by an amount proportional to the initial intensity I_0 and the thickness of the slice. We can thus write:

$$I(\Delta x) = I_0 - \alpha I_0 \Delta x$$

This can be recast into the form:

$$\frac{I(\Delta x) - I_0}{\Delta x} = -\alpha I_0 = \frac{dI}{dx}$$

which is a differential equation with the solution

$$I(x) = I_0 \exp(-\alpha x)$$

By convention, this Lambert-Beer law is usually written in decadic form:

$$I(x) = I_0 10^{-ax}$$

with the proportionality constant a = α/ln(10). The higher the concentration c of molecules in the sample, the larger is a. Writing a = ϵc obtain for the light intensity after a sample of thickness d:

$$I(d) = I_0 10^{-\epsilon c d}$$

The wavelength dependent quantity $\epsilon(\lambda)$ is called molar extinction coefficient. It is a measure of the probability that an electronic transition takes place when a molecule interacts with light of wavelength λ. By convention, the sample thickness d is given in cm, the concentration in mol/L. Consequently, the unit of ϵ is

$$[\epsilon] = \frac{\mathrm{L}}{\mathrm{mol\ cm}} = \mathrm{M}^{-1}\mathrm{cm}^{-1}$$

UV-visible spectrometers usually display the absorbance $A(\lambda)$, which is the negative log-ratio of transmitted (sample in beam) over incident (no sample in beam) intensities:

$$A(\lambda) = -\log_{10} \frac{I(d)}{I_0} = \epsilon(\lambda) c d$$

When more than one species with concentration c_i is present in the sample, the absorbance is the sum of the different contributions:

$$A(\lambda) = (\epsilon_1(\lambda) c_1 + \epsilon_2(\lambda) c_2 + \ldots)\, d$$

An absorption spectrum $A(\lambda)$ shows us the wavelength at which a molecule can absorb light and thus provides information about electronic state energies. Consequently, absorption spectroscopy in the UV-visible spectral region is sometimes called "electronic spectroscopy". From the magnitude of $A(\lambda)$ we can obtain information about sample composition or the probability of an electronic transition. Depending on the nature of the ground and excited state orbitals this probability can be very different.

3 CHAPTER THREE: MATERIALS AND METHODS

3.1 Equipment

The following equipment were used for this experimental work:

- Weighing Balance, 20ml beakers
- Spin Coating Machine
- Scanning Electron Microscope
- UV/VIS Spectrophotometer
- Hot plate
- Tweezers
- Bare glass and ITO coated glasses
- Magnetic stirrers
- Diamond cutter

3.2 Chemicals

- Chloroform
- Titanium dioxide powder
- MEHPPV powder
- Isopropanol
- Acetone
- Ethanol
- Deionized water.

3.3 Session one: Varying composition on bare glass

3.3.1 Bare glass

The glass slides, cut in sizes of 2 by 1.5cm were cleaned in detergent (in water) for 15 minutes; afterwards they were rinsed with deionized water for about 5minutes. The washed glass slides were placed in acetone for 15minutes followed by 15 minutes in ethanol at room temperature. The glass slides were dried by use of an electric pressure drier. However, these glasses were

sometimes left to dry at room temperature depending on the urgency of their application at a particular time. Glasses were carefully (for easy placement into the characterization machines) cut using a diamond cutter. They were many in number too for two reasons; percentages of composition were many (about six different compositions) and also substitutions in case of mess up of any of them. They were then kept in well cleaned and rinsed beakers or Petri dishes for use.

3.3.2 MEHPPV and Titanium dioxide

These two chemicals were used for deposition on the glass substrates. First, MEHPPV was spin coated alone and then various compositions of titanium dioxide were added to it in increasing steps.

3.3.3 One-step spin coating process

5 mg of MEHPPV was dissolved in 20ml of chloroform and stirred at 70^{o}C with the help of a magnetic stirrer for six hours to allow for complete dissolution and a transparent reddish solution was obtained. After thorough dissolving, at least three bare glass slides (with no coating of any kind) were spin coated with it for 40seconds at 4000rpm and annealed at 110^{o}C for 15minutes to allow for evaporation of the chloroform and then these glasses were taken for SEM and UV-Vis analyses for examination of optoelectronic properties and morphology observations. These coated glasses were seen having a thin red layer of MEHPPV dried on them

Varying compositions of TiO2 were also dissolved in Chloroform. 3 ml of chloroform were used for all compositions of tio2 and stirred for only 20minutes before dissolving in 3 ml of MEHPPV. Compositions of 0.1, 0.2, 0.3, 0.4 and 0.5g of TiO_2 were separately added and dissolved in 3 ml of MEHPPV (dissolved in Chloroform for six hours) by stirring for six hours. This gave a thick light-reddish solution. In the similar way, this thick solution of MEHPPV and TiO2 was deposited by spin coating on bare glass slides at 4000rpm for 40seconds in sets of eight for each composition owing to various techniques and possibilities of spoilage. They were annealed at 110^{o}C for the same reason as earlier mentioned.

The coated and annealed glass slides were then observed to have a thin light-reddish layer dried on their single sides ready for characterization. They were then taken for analysis.

3.4 Session two: ITO coated glass slides with varying TiO_2 composition

3.4.1 ITO coated glass slides

All preparations done in session one was repeated, only with different glasses coated with ITO for comparison of morphology and optoelectronic characteristics.

4 CHAPTER FOUR: RESULTS AND DISCUSSION

4.1 Morphology of MEH-PPV films on bare glass

4.1.1 SEM images

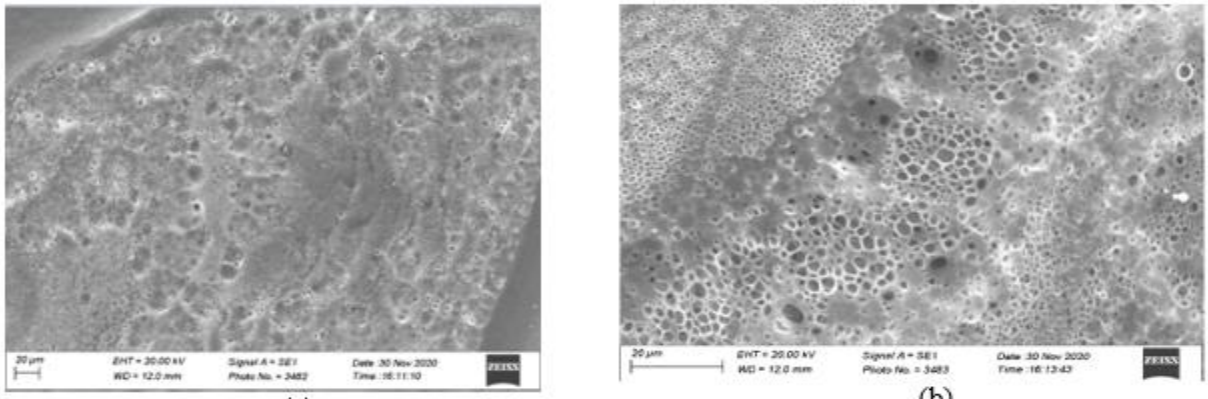

Figure 4.1: SEM images for Pure MEHPPV, (a) and Pure MEHPPV magnified, (b).

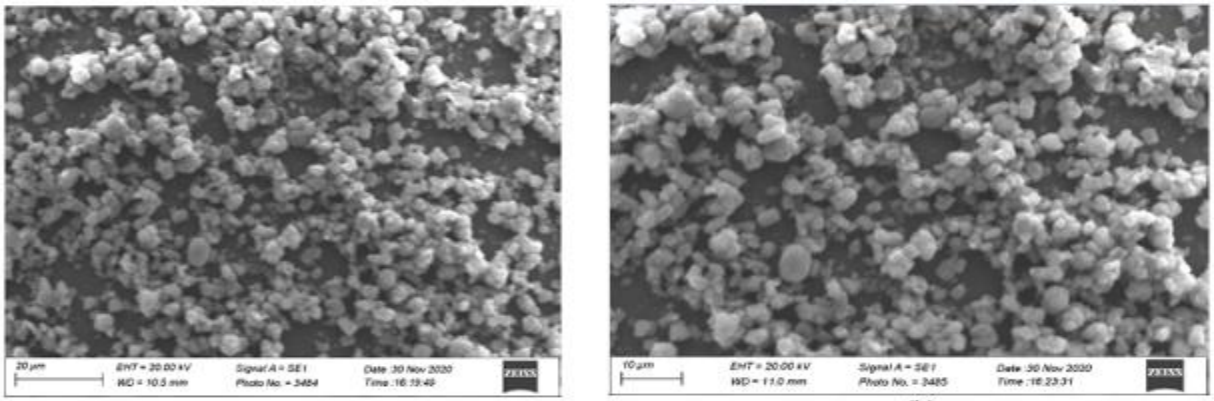

Figure 4.2: (a) 0.1g TiO2 in MEHPPV and (b) 0.1g TiO2 in MEHPPV Magnified

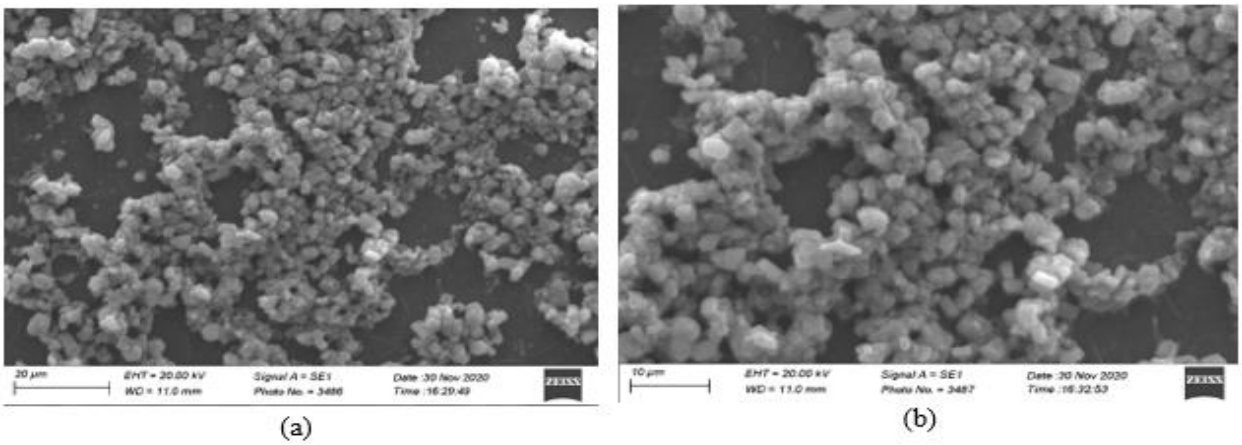

Figure 4.3: (a) 0.2g TiO2 in MEHPPV and (b. 0.2g TiO2 in MEHPPV magnified

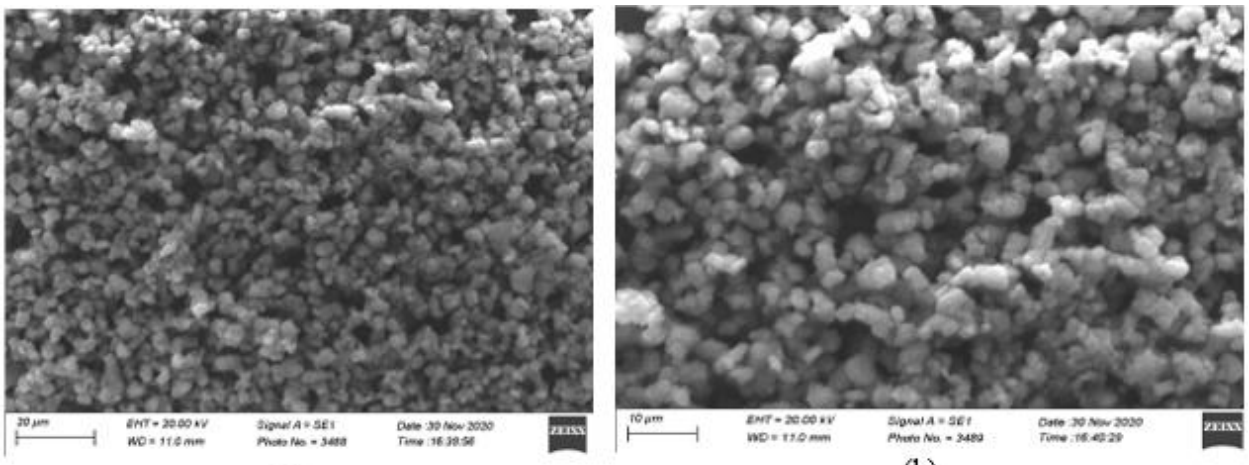

Figure 4.4: (a) 0.3g TiO2 in MEHPPV and (b) 0.3g TiO2 in MEHPPV magnified

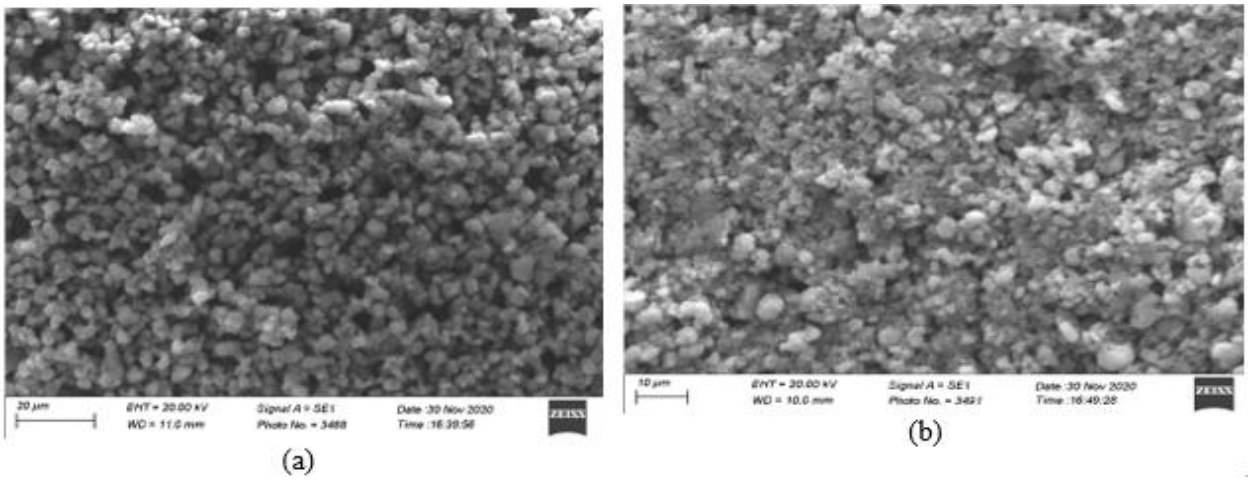

Figure 4.5: (a) 0.4g TiO2 in MEHPPV and (b) 0.4g TiO2 in MEHPPV magnified

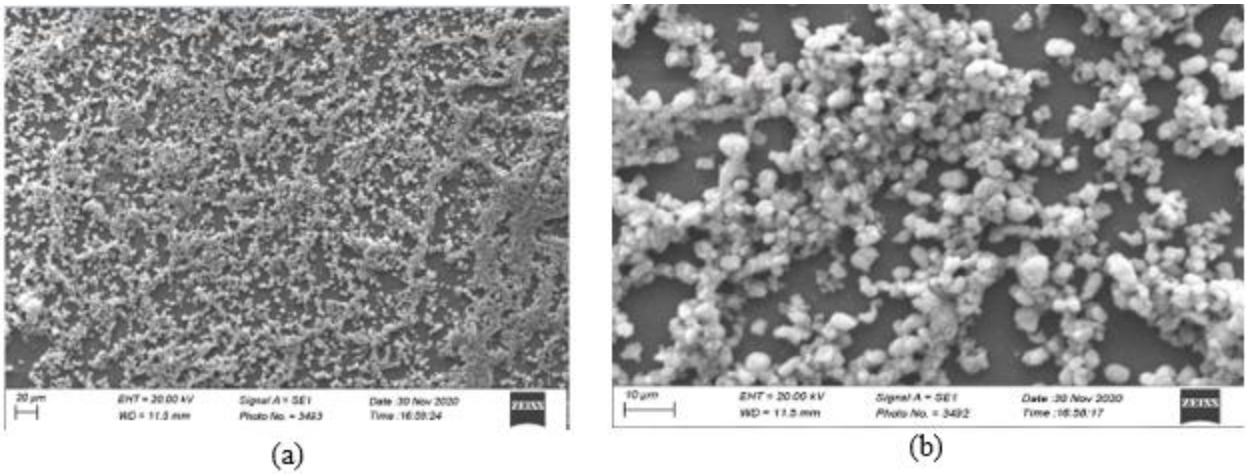

Figure 4.6: (a) 0.5g TiO2 in MEHPPV and (b) 0.5g TiO2 in MEHPPV magnified

From the SEM images we see above, increasing the percentage composition of TiO2 in the active layer MEHPPV increases the level of closure of the nanopores in the layer. Pure

MEHPPV image is seen to display pores of higher orders in magnitude than the other images in which TiO2 was incorporated. This trend, however, was seen to lose track when a certain composition was reached i.e. 0.4g(Fig. 5 a and b) leading to tighter closure of nanopores in particular regions and wider pores in the others. Three possible reasons might be responsible for this mess, in my opinion; too much infusion of TiO2 nanoparticles might not be good for improving the MEHPPV, nature of the glass and the possibility of mixing up percentage compositions during dissolving or labeling. This increase in closure of nanopores shortens the conjugation lengths in MEHPPV active layer for better optoelectronics performance.

4.2 Morphology of MEH-PPV films on FTO coated glass results

4.2.1 SEM images

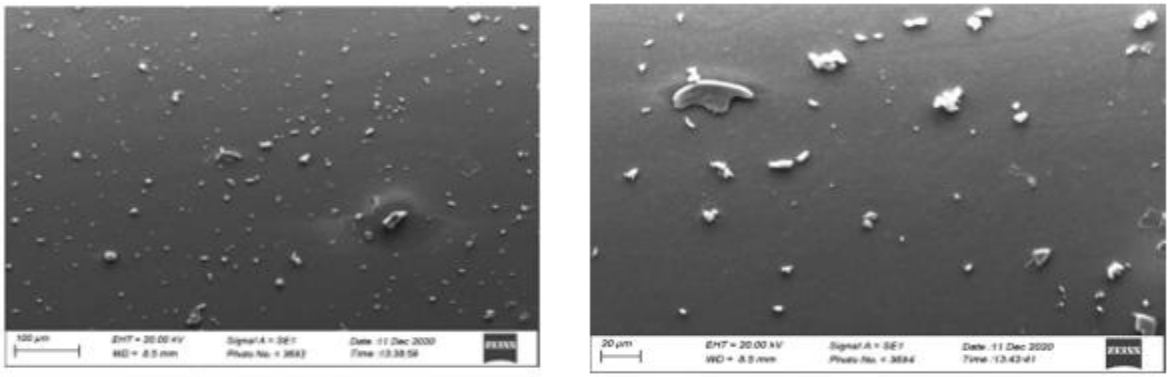

(a) (b)

Figure 4.7: (a) Pure MEHPPV on FTO glass and (b) Pure MEHPPV on FTO glass magnified

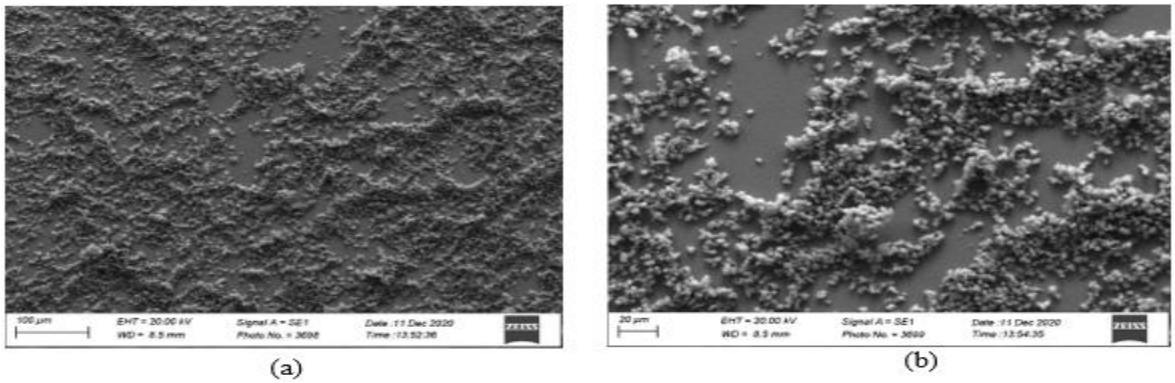

(a) (b)

Figure 4.8: (a) 0.1g TiO2 in MEHPPV on FTO and (b) 0.1g TiO2 in MEHPPV on FTO magnified

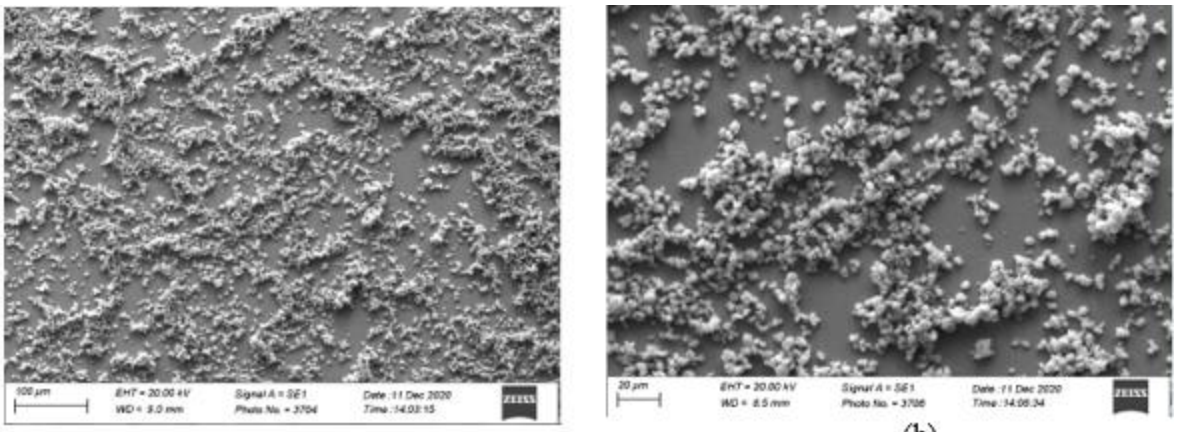

Figure 4.9: (a) 0.2g TiO2 in MEHPPV on FTO and (b) 0.2g TiO2 in MEHPPV on FTO magnified

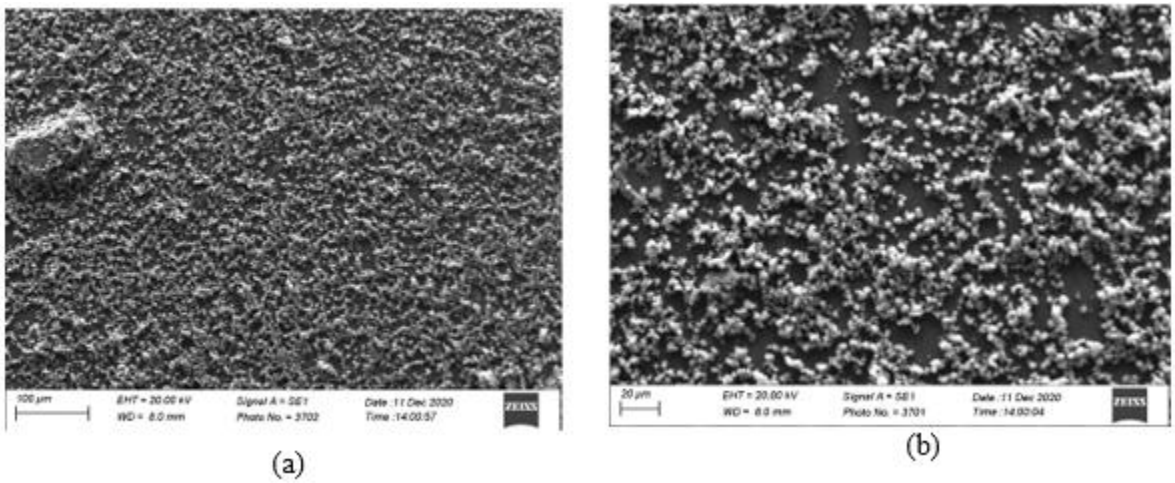

Figure 4.10: (a) 0.3g TiO2 in MEHPPV on FTO and (b) 0.3g TiO2 in MEHPPV on FTO magnified

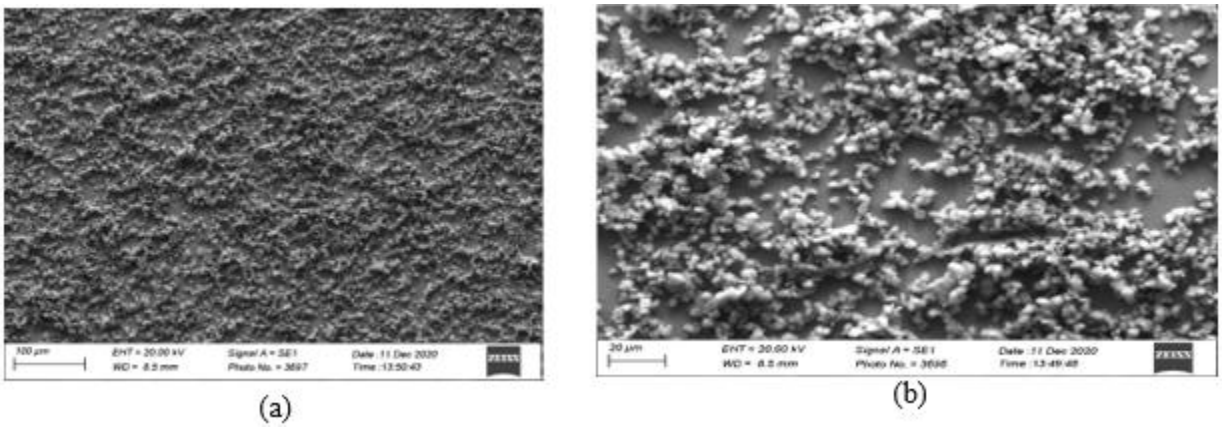

Figure 4.11: (a) 0.4g TiO2 in MEHPPV on FTO and (b) 0.4g TiO2 in MEHPPV on FTO magnified

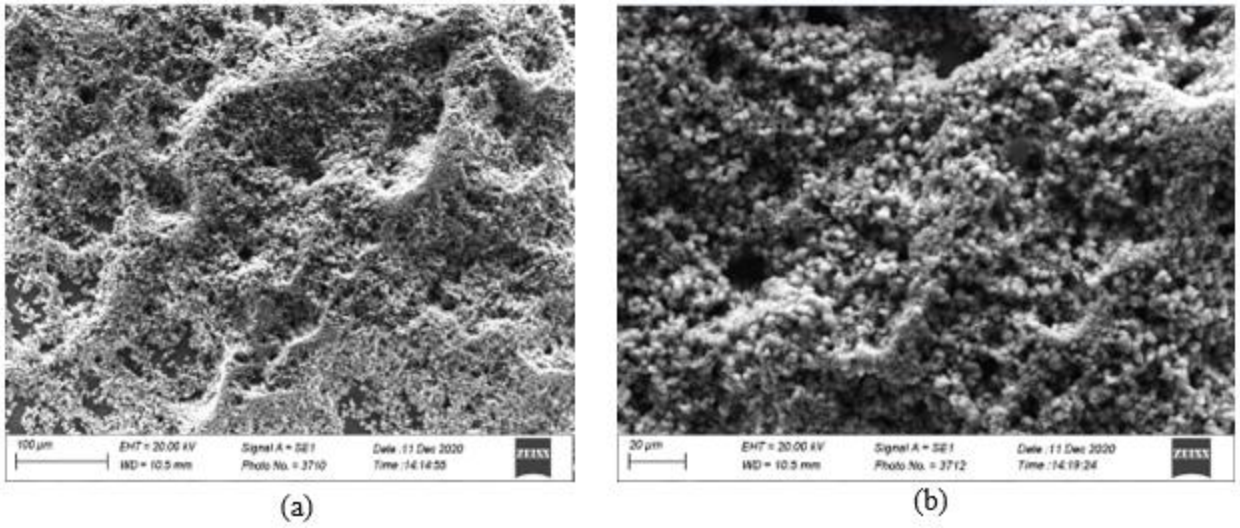

Figure 4.12: (a) 0.5g TiO2 in MEHPPV on FTO and (b) 0.5g TiO2 in MEHPPV on FTO magnified

The FTO coated glass results are as seen in the SEM images above. There is a slight improvement in the closure of the nanopores in the MEHPPV when glasses coated with FTO are used. However, contrary to the first case of bare glass, these results gave an improved morphology even for very high compositions of TiO2 in MEHPPV. This would probably answer the suspicion expressed in the bare glass case in which the type of glass might have contributed to the mess (to be further investigated). In fact, these morphological results show much better gap filling at high percentage compositions that at lower compositions. This can explain why the FTO coated glass may be a better option in attempts to improve morphology of MEHPPV active layer by the TiO2 nanoparticle infusion method for OLEDs applications. In a closer view of the dispersion of MEH-PPV and TiO2 combinations on these glasses, we see that they are smoother than the first glass type.

4.3 UV-VIS results

The thin films obtained with the similar deposition methods and procedures in the SEM images above were also used or inspected under the UV visible spectroscopy. All the percentage variations of TiO2 in MEH-PPV were analyzed and below are the results obtained through plots and their explanations.

4.3.1 MEH-PPV on FTO-coated glass

4.3.1.1 Absorbance graphs

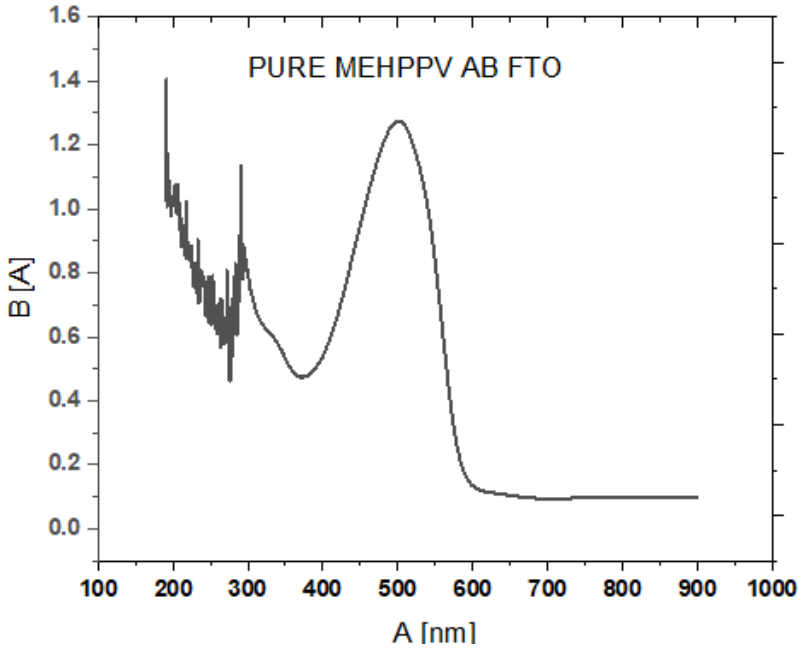

Figure 4.13: Pure MEH-PPV Absorbance plot

For this thin film of pure MEHPPV, the absorbance 1.3 $Lmol^{-1}cm^{-1}$ was found to be a peak at a wavelength of ~309nm. There was a noise tendency up to around a wavelength of 103nm.

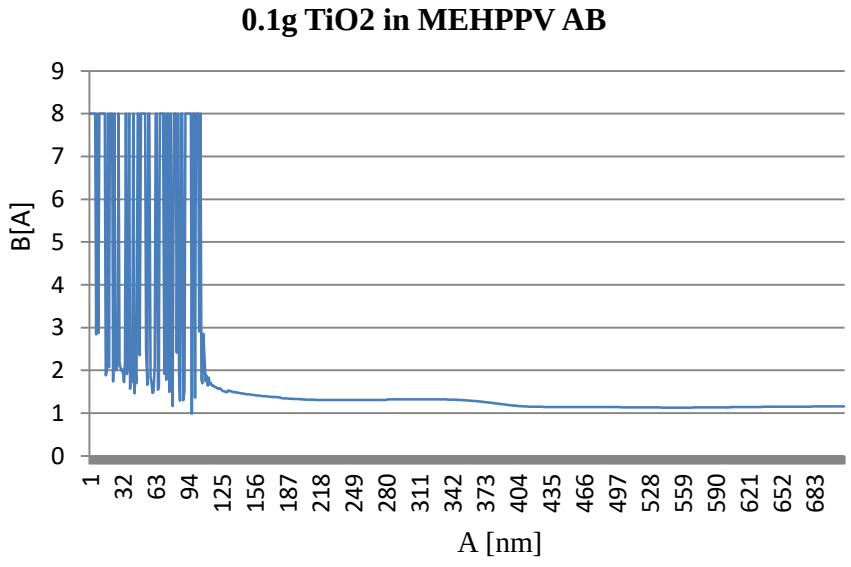

Figure 4.14: 0.1g TiO2 in MEH-PPV Absorbance plot.

When 0.1 g of TiO2 nanoparticles were infused in this MEHPPV, the absorbance was observed to shift to ~1.4 $Lmol^{-1}cm^{-1}$ in the wavelength range of 275nm-340nm. There was a slight increment in the absorbance value. Signal Noise was observed to go up to ~109nm.

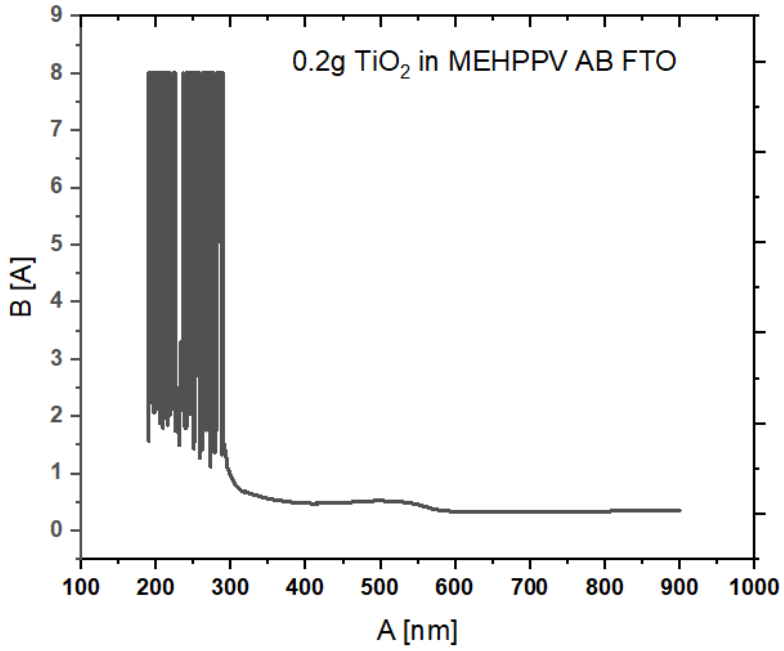

Figure 4.15: 0.2g TiO2 in MEH-PPV Absorbance plot.

An increament to 0.2g TiO2 yielded an absorbance of ~0.5 $Lmol^{-1}cm^{-1}$(smaller than the above) range of 300nm-320nm, implying the wavelength range just reduced and was narrower. Also the noise reduced to stop around 93nm.

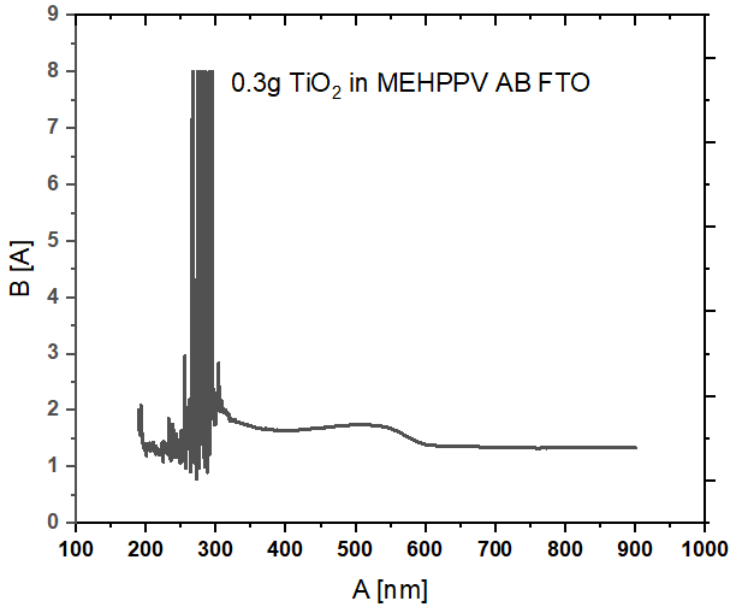

Figure 4.16: 0.3g TiO2 in MEH-PPV Absorbance plot.

0.3g TiO2 in MEHPPV produced an absorbance value of ~1.9 Lmol-1cm-1(higher than the above two) within the wavelength range of 279nm-346nm(wider) with a signal noise stopping at about 106nm.

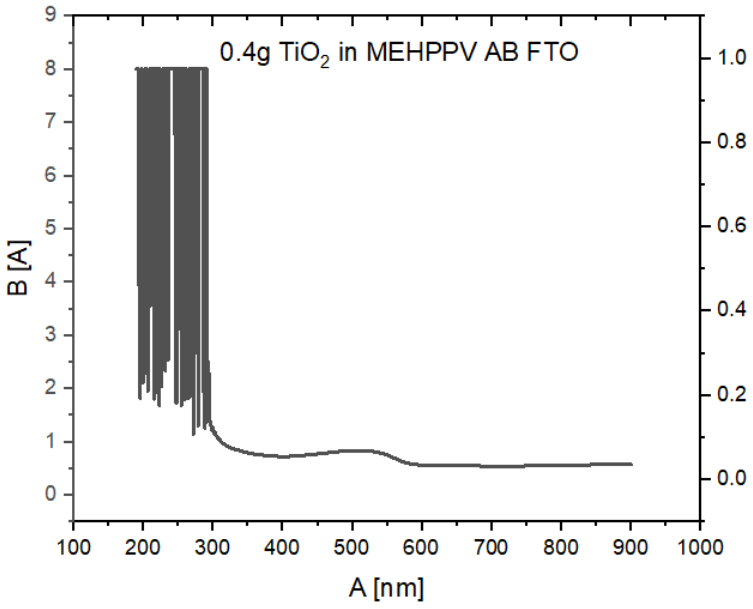

Figure 4.17: 0.4g TiO2 in MEH-PPV Absorbance plot.

0.4g TiO2 addition led to a signal noise limit of up about 100nm with peak absorbance of ~0.9 $Lmol^{-1}cm^{-1}$ in the wavelength range of 270nm-348nm. This was relatively a wider absorbance range, though absorbance reduced.

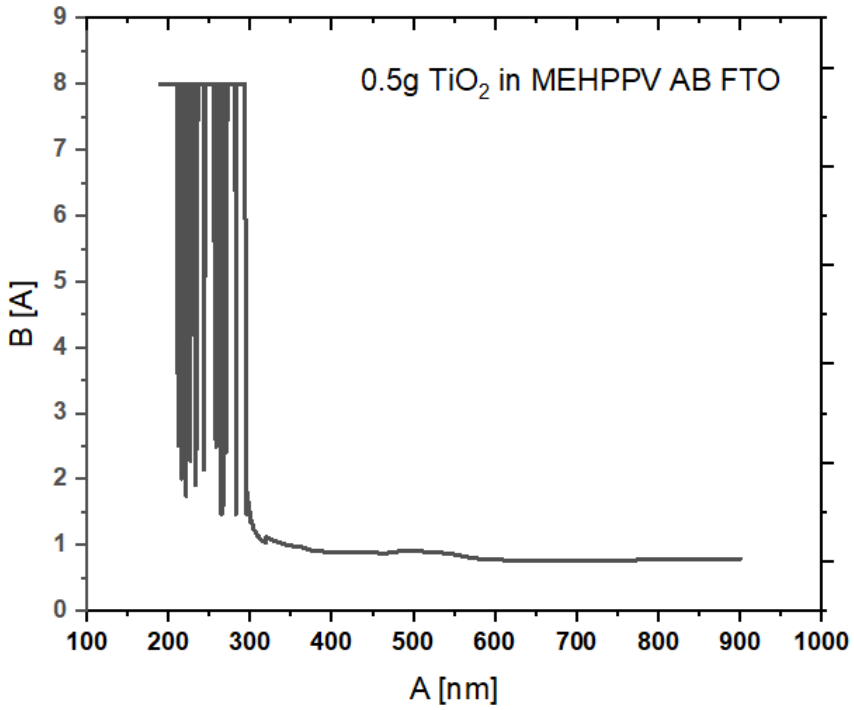

Figure 4.18: 0.5g TiO2 in MEH-PPV Absorbance plot.

0.5g in TiO2 in MEHPPV was found to give a maximum wavelength of ~0.95 $Lmol^{-1}cm^{-1}$ within the wavelength range of 280nm-330nm with a signal noise ending at close to 100nm.

We notice, in general, that the absorbance was maximized at the moderate concentration of TiO2 (0.3g) in MEHPPV. It is seen that low and high concentrations gave absorbance values lower than the pure MEHPPV. Therefore, one would recommend moderate infusion.

4.3.1.2 Transmittance graphs

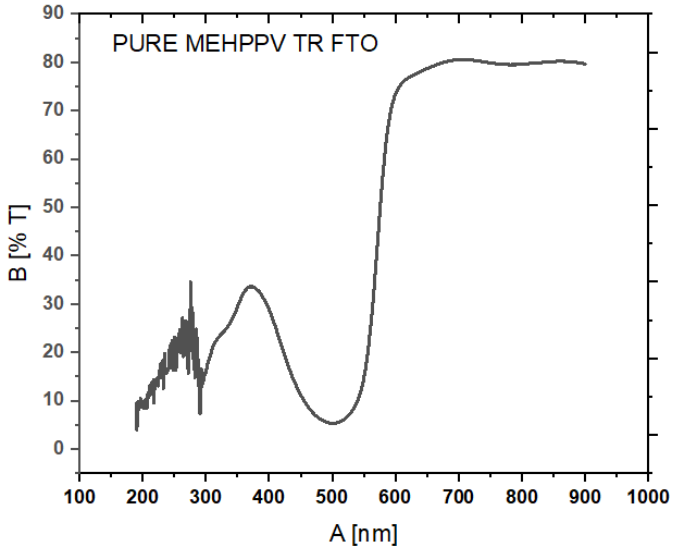

Figure 4.19: Pure MEH-PPV Transmittance plot.

A pure MEHPPV thin film was observed to give the first maximum transmittance of 34 at 185nm wavelength and then 80 at 461nm whereas the minimum transmittance of 5 was observed to be at a wavelength of 314nm. Better transmittance is thus found at wavelengths greater or equal to 460nm.

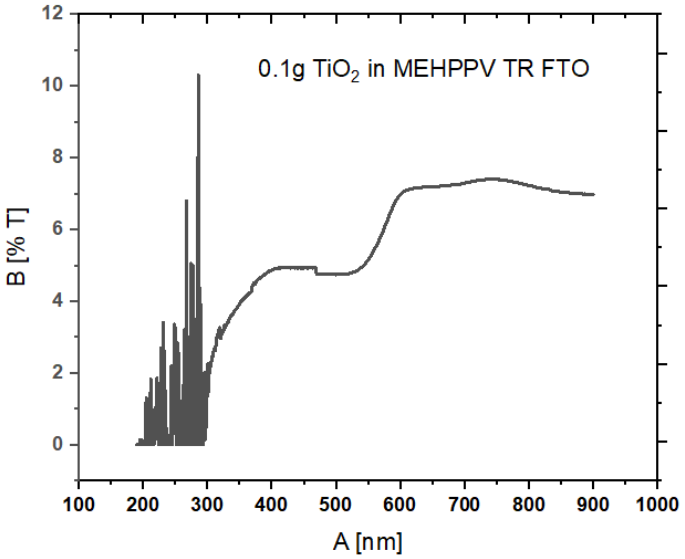

Figure 4.20: 0.1g TiO2 in MEH-PPV Transmittance plot.

When 0.1g TiO2 was infused, we observed the first maximum transmittance of 5 in a wavelength range of 208nm-277nm and the second maximum transmittance of 7.5 occurring at 530nm and above. The minimum here was seen to be at ~4.8 within a wavelength range of 280nm-330nm.

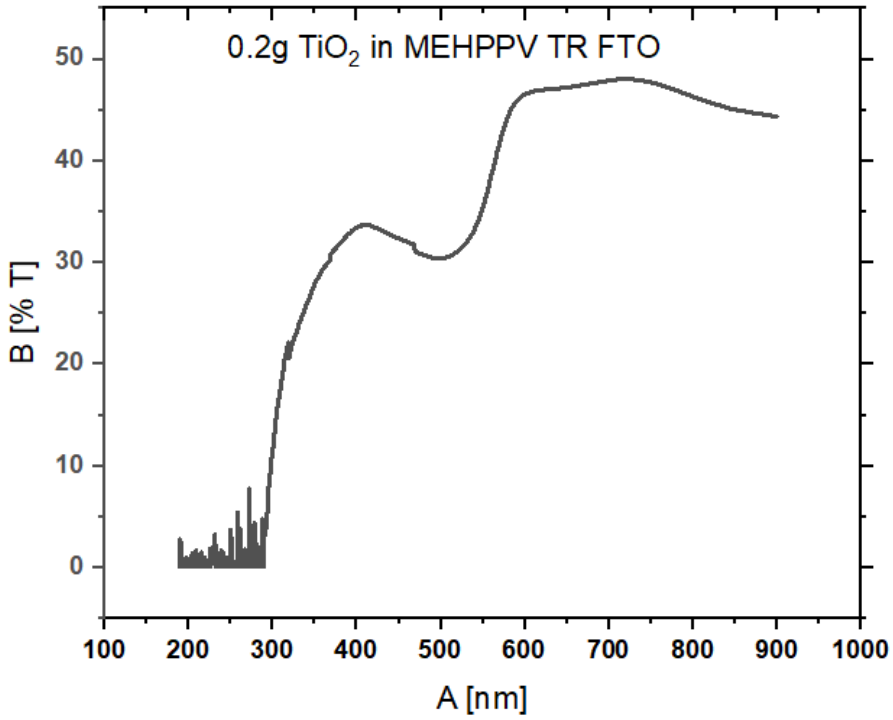

Figure 4.21: 0.2g TiO2 in MEH-PPV Transmittance plot.

When 0.2g TiO2 was incorporated, we observed the first maximum transmittance of 34 at a wavelength of 220nm and the second maximum transmittance of ~48 occurring at 507nm and above. The minimum here was seen to be at 30 within a wavelength range of 298nm-320nm.

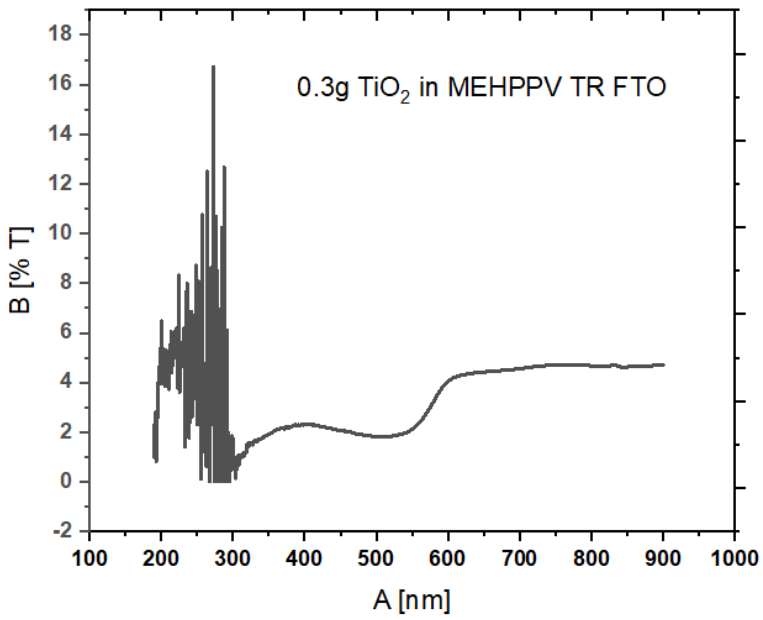

Figure 4.22: 0.3g TiO2 in MEH-PPV Transmittance plot.

When 0.3g TiO2 was now infused, we observed the first maximum transmittance of 2.3 at a wavelength of 210nm and the second maximum transmittance of ~4.8 occurring at 530nm and above. The minimum here was seen to be at 2 within a wavelength range of 250nm-350nm.

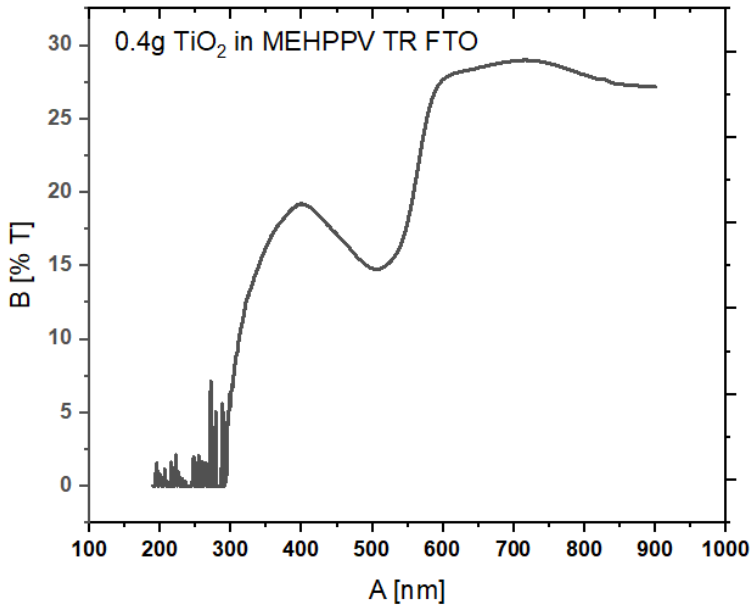

Figure 4.23: 0.4g TiO2 in MEH-PPV Transmittance plot.

When 0.4g TiO2 was incorporated, we observed the first maximum transmittance of 19 at a wavelength of 204nm and the second maximum transmittance of ~29 occurring at 507nm within 496nm-541nm wavelength range. The minimum here was seen to be at 14.9 at a wavelength of 316nm.

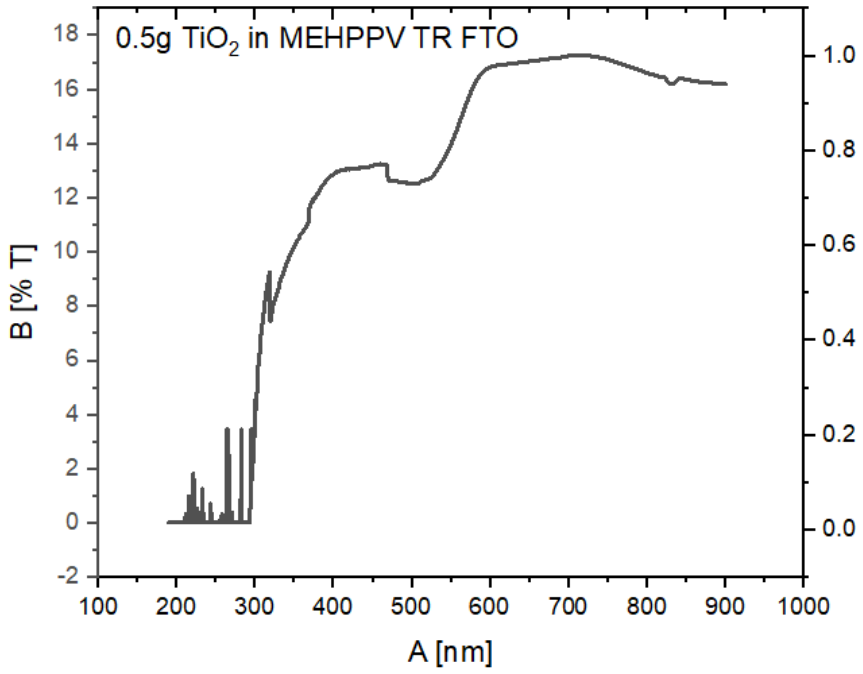

Figure 4.24: 0.5g TiO2 in MEH-PPV Transmittance plot.

When 0.5g TiO2 was incorporated, we observed the first maximum transmittance of ~13.2 within a wavelength range of 248nm-267nm and the second maximum transmittance of ~17.3 occurring within a wavelength range of 514nm-533nm. The minimum in this case was seen to be at 12.5 at wavelength of 310nm.

We note, in general, that all signal noise effects were truncated at a wavelength of about 99nm in all compositions. It is clearly seen that best transmittance effects were felt at high percentage compositions of TiO2 in MEHPPV. One can then opt for high compositions for optimum transmittance of the MEHPPV layer in OLED applications.

4.3.2 MEH-PPV on bare glass

4.3.2.1 Absorbance graphs

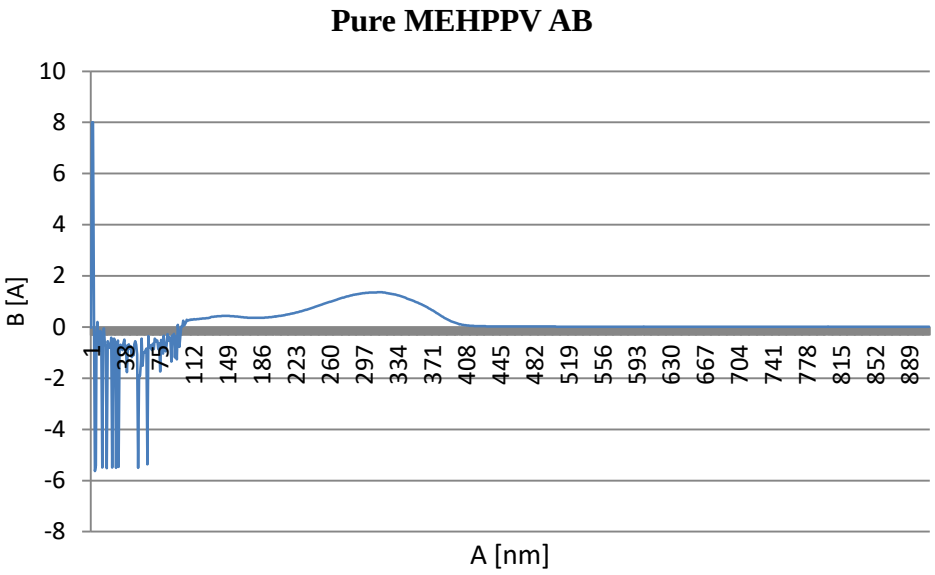

Figure 4.25: Pure MEH-PPV Absorbance plot.

For this thin film of pure MEHPPV, the absorbance 1.4 $Lmol^{-1}cm^{-1}$ was found to be a peak within a wavelength range of 300nm-324nm. There was a noise tendency up to around a wavelength of 96nm.

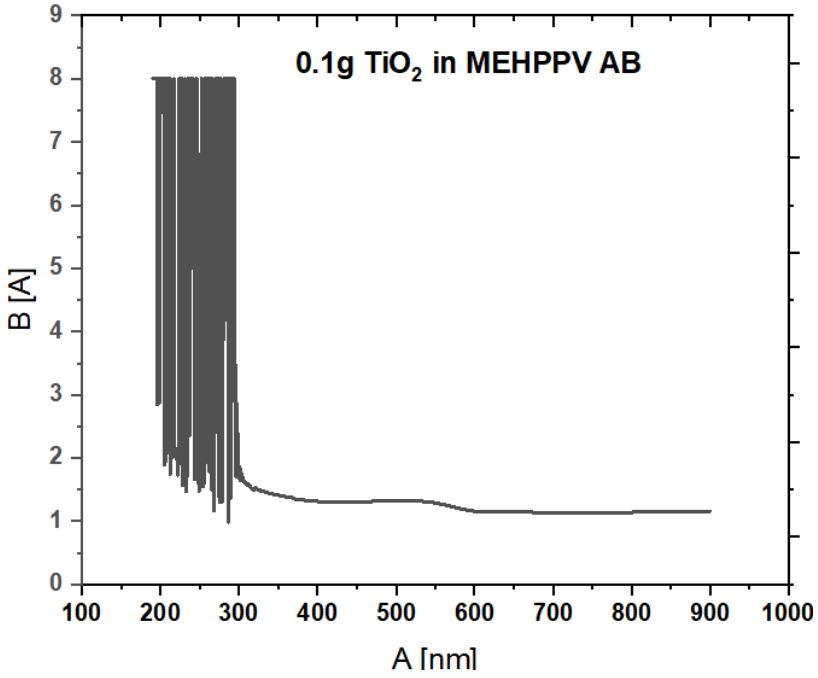

Figure 4.26: 0.1g TiO2 in MEH-PPV Absorbance plot.

0.1g TiO2 in MEHPPV produced an absorbance value of ~1.9 $Lmol^{-1}cm^{-1}$ within the wavelength range of 300nm-345nm with a signal noise extending up to about 105nm.

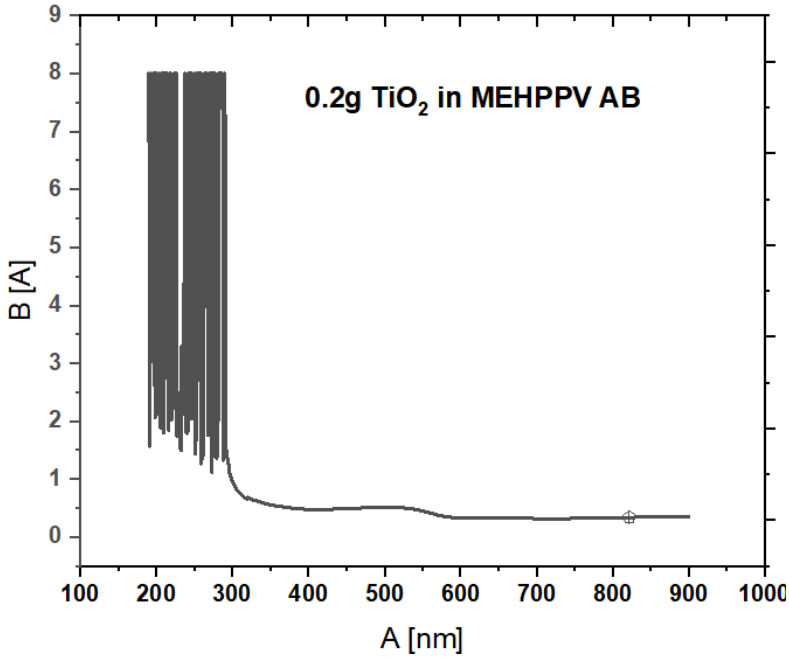

Figure 4.27: 0.2g TiO2 in MEH-PPV Absorbance plot.

When 0.2g TiO2 was infused in MEHPPV, it produced an absorbance value of ~0.5 $Lmol^{-1}cm^{-1}$ and flattened from a wavelength of 103nm onwards with a signal noise stopping at the same wavelength.

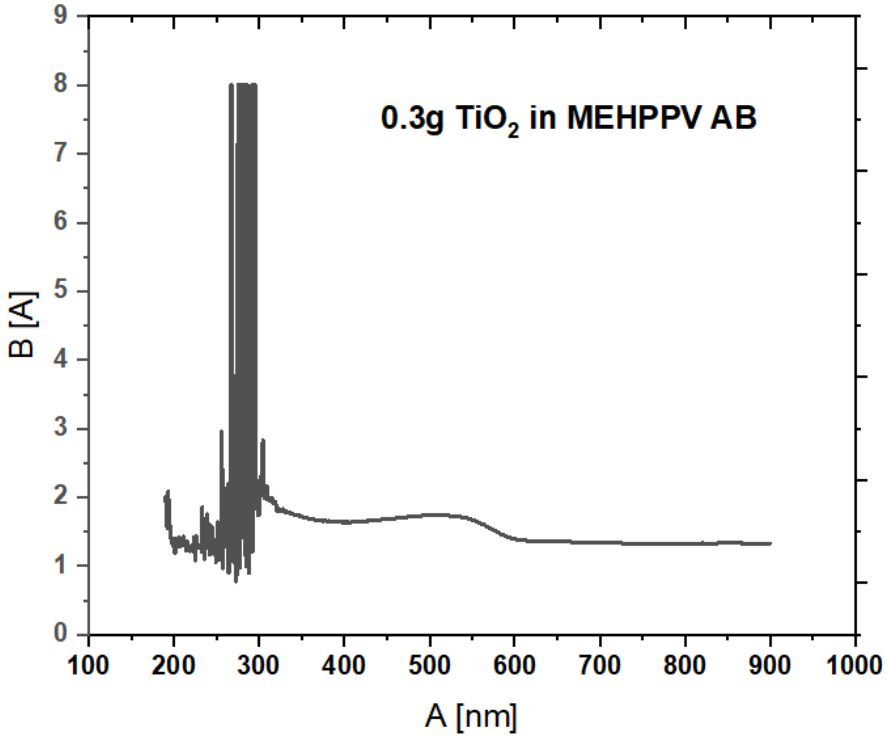

Figure 4.28: 0.3g TiO2 in MEH-PPV Absorbance plot.

0.3g TiO2 in MEHPPV produced an absorbance value of ~1.1 $Lmol^{-1}cm^{-1}$ within the wavelength range of 278nm-353nm with a signal noise extending up to about 105nm.

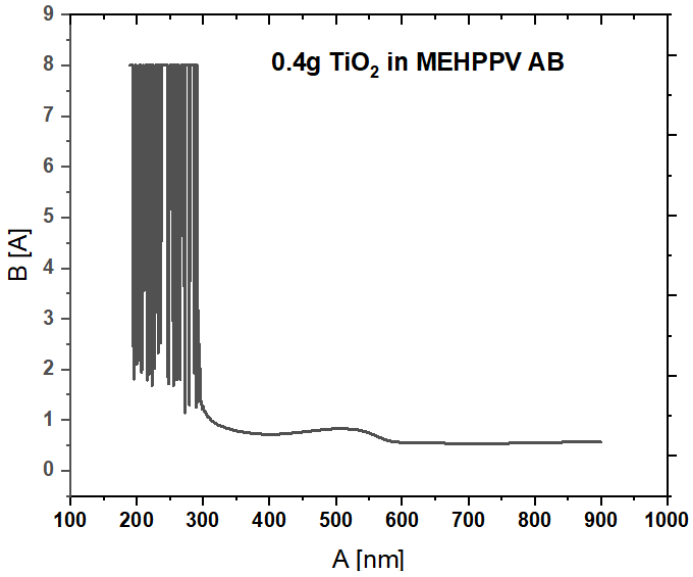

Figure 4.29: 0.4g TiO2 in MEH-PPV Absorbance plot.

When we increased to 0.4g TiO2 in MEHPPV, we obtained a peak absorbance value of ~1.35 $Lmol^{-1}cm^{-1}$ within the wavelength range of 267nm-362nm with a signal noise extending up to about 105nm.

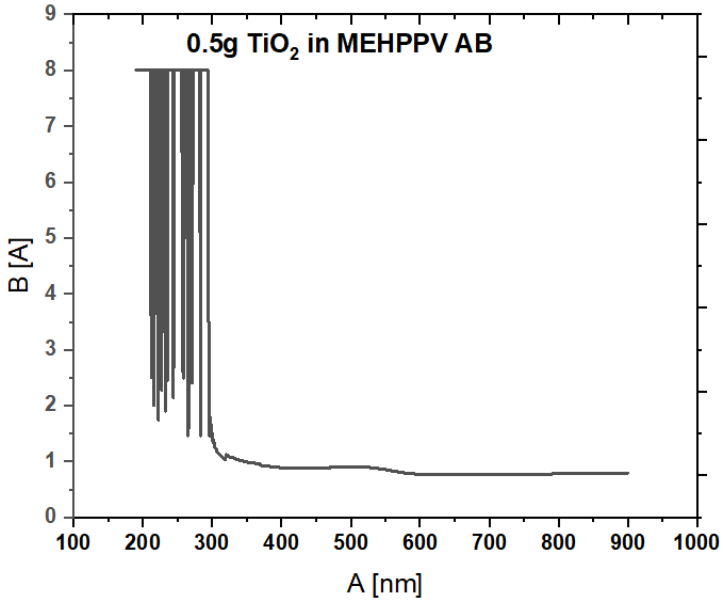

Figure 4.30: 0.5g TiO2 in MEH-PPV Absorbance plot.

0.5g TiO2 in MEHPPV produced an absorbance value of ~1.5 $Lmol^{-1}cm^{-1}$ within the wavelength range of 345nm-375nm with a signal noise extending up to about 105nm.

4.3.2.2 Transmittance graphs

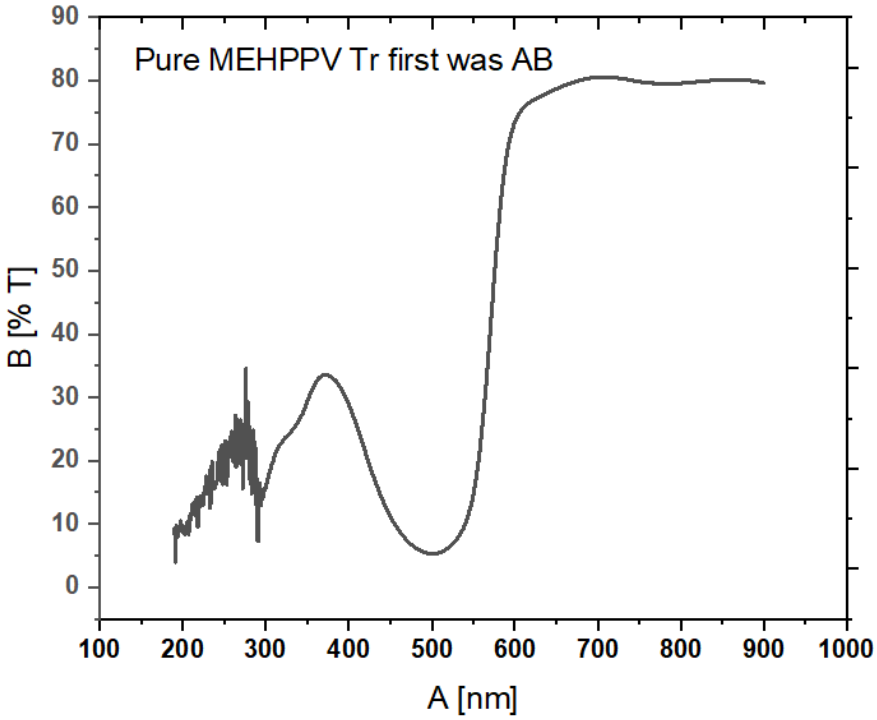

Figure 4.31: Pure MEH-PPV Transmittance plot.

A pure MEHPPV thin film was observed to give the first two sharp linear peaks at wavelengths between 38nm and 75nm and then flattened at zero for the rest of the wavelengths. The peaks stand at transmittances of $2.2x10^7$ and $3.1x10^7$.

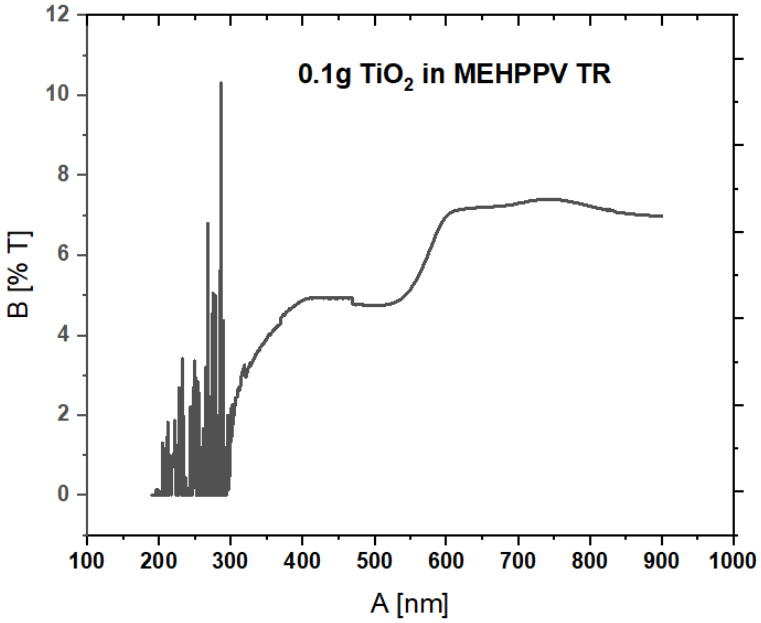

Figure 4.32: 0.1g TiO2 in MEH-PPV Transmittance plot.

When 0.1g TiO2 was incorporated, a thin film was observed to give the first two sharp linear peaks at wavelengths 19nm and 57nm and then flattened at zero for the rest of the wavelengths. The peaks stand at transmittances of $6.1x10^6$ and $4.5x10^6$.

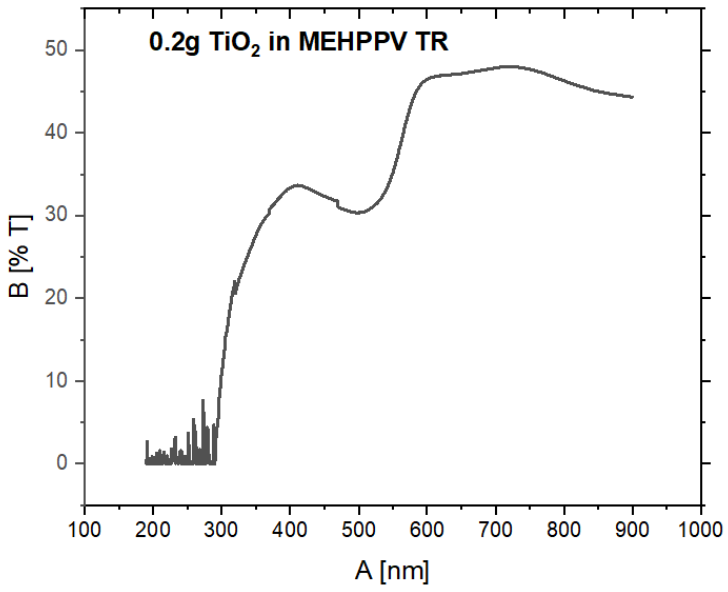

Figure 4.33: 0.2g TiO2 in MEH-PPV Transmittance plot.

On infusing 0.2g TiO2 in MEHPPV thin film, it was observed to give the first three sharp linear peaks at wavelengths 20nm, 25nm and 55nm and then flattened at zero for the rest of the wavelengths. The peaks stand at transmittances of $7.5x10^6$, $7.5x10^6$ and $4.0x10^6$.

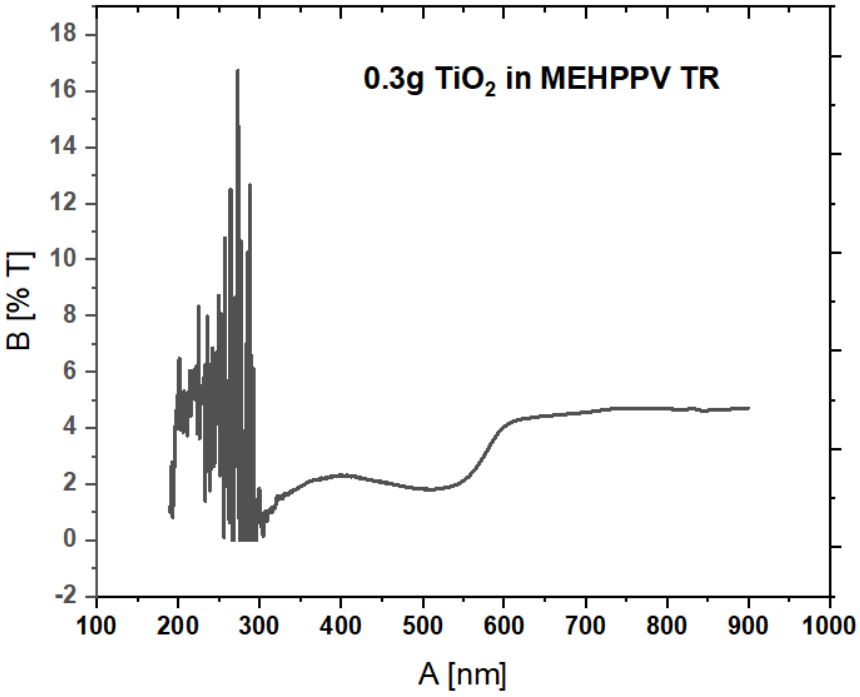

Figure 4.34: 0.3g TiO2 in MEH-PPV Transmittance plot

On infusing 0.3g TiO2 in MEHPPV, it was observed to give the first maximum transmittance of 8.5 at a wavelength 298nm and the second maximum transmittance of 10 at the wavelength of 545nm and onwards. The minimum transmittance of 7.1 is observed to be at a wavelength of 324nm. The signal noise was terminated at a wavelength of about 115nm.

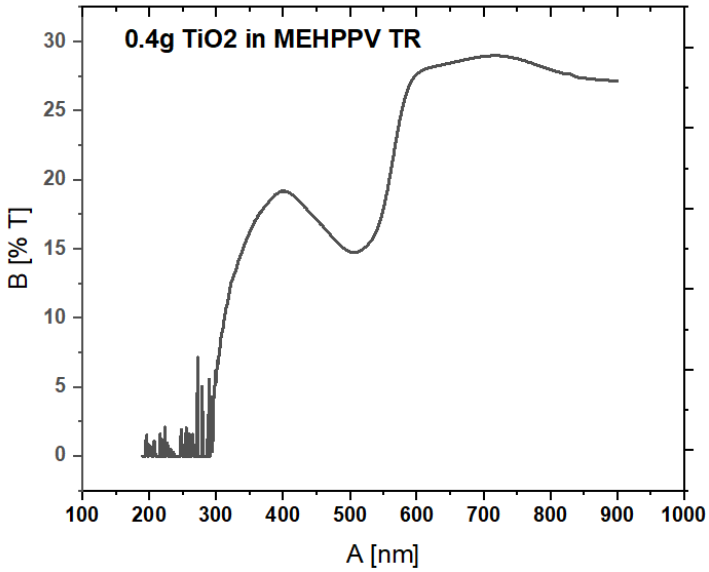

Figure 4.35: 0.4g TiO2 in MEH-PPV Transmittance plot.

On infusing 0.4g TiO2 in MEHPPV, it was observed to give the first maximum transmittance of 8.0 at a wavelength 175nm and the second maximum transmittance of 9.8 at the wavelength of 540nm and onwards. The minimum transmittance of 5.4 is observed to be within a wavelength range of 290nm-350nm.

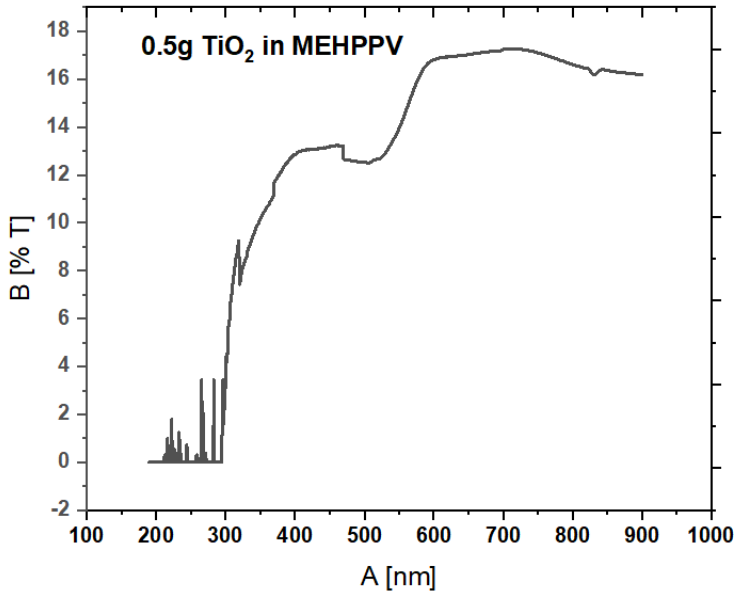

Figure 4.36: 0.5g TiO2 in MEH-PPV Transmittance plot.

0.5g TiO2 infusion into MEHPPV yielded a thin film whose transmittance graph came as above. First two sharp peaks were observed at wavelengths of 70nm and 80nm with transmittance peak values of 2.0x105 and 1.31x107 respectively. The wavelengths beyond had flat(zero) transmittance. As much as noise effects were seen to moderate for bare glass, the transmittance effects were not as significant and good as those of the FTO coated glass. There is a general improvement in the percentage of intensity transmitted for the FTO coated glass type as compared to the bare glass. We observe a better electronic transition probability from the comparison of the bare glass and the one coated with FTO material. The absorption wavelengths correspond to the energy needed for excitation of electrons between energy levels. The lower the wavelength is the better the materials ability to allow for electron transition between the layers and the larger the range of the peak, the better the electron and hole transport efficiency. This is evident from the table of wavelengths for the two glass types above. In fact, this is true for transmission. It is seen that “flats” are more for the bare glass and none for the FTO, a clear indicative of better transmittance when the FTO glass is used rather than the bare glass. Consistence at the same time, for these values is less significant in the bare glass section as opposed to the FTO coated glass type.

5 CHAPTER FIVE: CONCLUSIONS AND FUTURE WORK.

5.1 Conclusions

In this work, we have deposited organic: inorganic thin films using poly [2-methoxy 5-(2'-ethyl-hexyloxy)-1, 4-phenylene vinylene] (MEH-PPV) polymer as electron donator with titanium dioxide (TiO_2) acting as an electron acceptor, by spin-coating deposition technique. We have investigated at 0.1g, 0.2g, 0.3g, 0.4g and 0.5g of TiO_2 composition effects on electrical, photoconductivity and optical properties of the nanocomposite MEH-PPV: TiO_2 thin films. SEM images and optical characteristics (UV-VIS, for instance) of the thin films found that the composition of TiO_2 in MEH-PPV might optimize the nanocomposite thin films performance. For optimum thin film performance, composition of TiO_2 at0.4g TiO2 gives the best morphological and photoconductivity properties. Whilst for optical properties, at 0.2g and 0.3g TiO2 shows an optimum absorbance with MEH-PPV and TiO_2 exhibited strong absorption at wavelength of ~320 nm in UV visible range. It is conjectured that by introduced TiO_2 nanoparticle in MEH-PPV matrices, it could lead to significant improvement in photoconductivity and optical characteristics for organic photovoltaic cell applications.

This research has focused on improving the morphology and optoelectronic properties of MEHPPV as an active layer for OLED applications. Two types of glasses were used, that is; the bare glass and the FTO coated glass. Same composition variation was done for both the glass types. We used 3ml to dissolve 0.1, 0.2, 0.3, 0.4, and 0.5g of TiO2 into 3ml MEH-PPV**.** SEM and UV-VIS techniques were then employed for characterization. From the SEM images we observe that the uniformity and roughness of the morphology was improving whenever the composition of TiO2 was increased. More pores were seen developing with better uniformity. This communicates those technical increments of TiO2 in MEH-PPV enhances the morphological properties for better absorption, absorbance and hence performance for OLED applications. We, however, note that the trend was lost for the bare glass case which might suggest that the use of FTO coated glass is the better option. But also, the error might have occurred in the process of mixing and so extra caution should be taken when next mixing. There was also a problem of high temperatures which affected the dissolving processes. The time chosen for the complete dissolution (as from literature) might have been too long. This is because solution samples were found dried due to high temperatures coupled with long hours of

dissolving. This led to multiple dissolution processes which might have had an effect on the overall results.

5.2 Future work

5.2.1 MEHPPV and TiO2

In this work, we have deposited organic: inorganic thin films using poly [2-methoxy 5-(2'-ethyl-hexyloxy)-1, 4-phenylene vinylene] (MEH-PPV) polymer as electron donator with titanium dioxide (TiO_2) acting as an electron acceptor, by spin-coating deposition technique. We have investigated at 0.1g, 0.2g, 0.3g, 0.4g and 0.5g of TiO_2 composition effects on electrical, photoconductivity and optical properties of the nano composited MEH-PPV: TiO_2 thin films. SEM images and optical characteristics (UV-VIS, for instance) of the thin films found that the composition of TiO_2 in MEH-PPV might optimize the nano composited thin films performance. For optimum thin film performance, composition of TiO_2 at0.4g TiO2 gives the best morphological and photoconductivity properties. Whilst for optical properties, at 10 wt.% shows an optimum absorbance with MEH-PPV and TiO_2 exhibited strong absorption at wavelength of 320 nm in UV visible range. It is conjectured that by introduced TiO_2 nanoparticle in MEH-PPV matrices, it could lead to significant improvement in photoconductivity and optical characteristics for organic photovoltaic cell applications.

This work triggers a lot of fields to be explored in OLED devices and solar energy field in general. There is need to investigate the variation of mechanical properties with composition using the Nanoindentation technique. This will be aimed at identifying the best percentage composition that yields the best mechanical properties of MEH-PPV as an active layer for OLED applications without compromising on other useful optoelectronic properties. This will enable us to choose the best quality combination of the active layer for OLED applications. Secondly, we aim to look at the sheet resistance of the thin films for application in solar cell devices. The experiments carried out herein need to be also carried out under improved conditions such as better temperatures and time of dissolving. Even the spin coating speed and annealing temperatures might be differently explored.

5.2.2 Perovskite Solar Cells

A lot of research is going on and the attention of many researchers has been taken by the need to improve the power conversion efficiencies of Perovskite solar cells by use of various techniques and innovations. However, there is a sincere observation of gaps in this field which need to be explored in further research studies. The versatility in the fabrication techniques of the Perovskite light-absorbing layer, which include the solution-deposition method, vapour-deposition method, and the vapour-assisted solution method, is attractive and such methods are also discussed in various experiments.

Perovskite solar cells have developed rapidly, but some critical factors may restrict the development of Perovskite solar cells. Firstly, the stability of the organic lead halide Perovskite is greatly affected by external environmental factors (such as humidity, temperature, and ultraviolet radiation), which lead to the low stability of the devices and the great difficulties in encapsulating cells in the later stage. Therefore, the development of a high-stability device composition, including the light-absorbing layer, electron/hole transport layer, and electrode materials, as well as the development of a simple and effective device-packaging method, will be of great significance to promote the practicability of such devices. Secondly, the hole transporting material Spiro-OMeTAD used in perovskite solar cells is very expensive (10 times the market price of gold) and its synthesis process is complex. Therefore, it is necessary to design and synthesize new hole transport materials to promote commercial applications of Perovskite solar cells. Thirdly, it is difficult to deposit a large area of continuous Perovskite film with the traditional methods described above and so other methods should be improved to prepare high-quality and large-area Perovskite solar cells for commercial production in the future. Fourthly, the Lead (Pb) element employed in Perovskite solar cells is highly toxic, which will hinder the industrial promotion and development of Perovskite solar cells. Therefore, it is necessary to find a low-toxicity or nontoxic ingredient to replace Pb in the future. Fifthly, there is a lack of deep understanding of the microscopic physics mechanism of Perovskite solar cells. Therefore, it is necessary to establish a complete theoretical model to explain the reasons for the increase in the conversion efficiency. Theoretical studies will not only help to further improve the performance of Perovskite solar cells but also provide ideas to develop simpler and/or more efficient new materials and structures.

Summarily, all the above issues need to be addressed before making full application of the MEH-PPV as an active layer and Perovskite solar cells technology.

REFERENCES.

A. De Caro, C. (2015). UV / VIS Spectrophotometry. *Mettler-Toledo International*, *September 2015*, 1–53.

Ahmed, M. I., Habib, A., & Javaid, S. S. (2015). Perovskite Solar Cells : Potentials , Challenges , and Opportunities. *International Journal of Photometry*, *2015*, 1–13. https://doi.org/10.1155/2015/592308

Al-asbahi, B. A. (2018). Influence of SiO 2 /TiO 2 Nanocomposite on the Optoelectronic Properties of PFO/MEH-PPV-Based OLED Devices. *Journal of Polymers*, 1–7. https://doi.org/10.3390/polym10070800

Al-asbahi, B. A. (2021). Enhancing the Optical and Optoelectronic Properties of MEH-PPV-Based Light-Emitting Diodes by Adding SiO 2 / TiO 2 Nanocomposites. *Journal of Non-Crystalline Solids*, *552*(September 2020), 120429. https://doi.org/10.1016/j.jnoncrysol.2020.120429

Al-asbahi, B. A., Qaid, S. M. H., Ha, M., Jumali, H., Alsalhi, M. S., & Aldwayyan, A. S. (2019). Long-range dipole – dipole energy transfer enhancement via addition of SiO 2 / TiO 2 nanocomposite in PFO / MEH-PPV hybrid thin fi lms. *Journal of Applied Polymer Science*, *47845*, 1–11. https://doi.org/10.1002/app.47845

Bastiani, M. De. (2016). *Ph . D . Thesis : The stability of third generation solar cells Università degli Studi di Padova*. *October*.

Chergui, Y., Nehaoua, N., & E., D. (2011). Comparative Study of Dye-Sensitized Solar Cell Based on ZnO and TiO2 Nanostructures. *Solar Cells - Dye-Sensitized Devices*. https://doi.org/10.5772/21452

Dinh, N. N., Chi, L. H., Long, N. T., Thuy, T. T. C., Trung, T. Q., & Kim, H.-K. (2009). Preparation and characterization of nanostructured composite films for organic light emitting diodes. *Journal of Physics*, 1–8. https://doi.org/10.1088/1742-6596/187/1/012029

Dinh Van, C., & Dinh Van, T. (2015). The MEH-PPV/YAG:Ce Hybrid Nanocomposite Material for Solution Processing Fabrication of Optoelectronic Device. *Journal of Nanomaterials*, *2015*. https://doi.org/10.1155/2015/313472

Han, J., Bao, F., Wang, X., Bao, X., Han, J., Bao, F., Wang, X., Huang, D., Yang, R., & Yang, C. (2021). Article Identifying tunneling effects of poly (aryl ether) matrices and boosting the efficiency , stability , and stretchability of organic solar cells matrices and boosting the efficiency , stability ,. *Cell Reports Physical Science*, *2*(5), 100408. https://doi.org/10.1016/j.xcrp.2021.100408

Hieu, N. H. (2012). Graphene-Based Material for Fabrication of Electrodes in Dye-Sensitized

Solar Cells. *Intechopen*, 13. http://dx.doi.org/10.1039/C7RA00172J%0Ahttps://www.intechopen.com/books/advanced-biometric-technologies/liveness-detection-in-biometrics%0Ahttp://dx.doi.org/10.1016/j.colsurfa.2011.12.014

Hou, W., Xiao, Y., Han, G., & Lin, J. Y. (2019). The applications of polymers in solar cells: A review. *Polymers*, *11*(1), 1–46. https://doi.org/10.3390/polym11010143

Ibrahim, I. M., & Sharhan, S. I. (2019). Enhancement of MEH-PPV by introducing anatase TiO2 nanoparticles for oled device. *Digest Journal of Nanomaterials and Biostructures*, *14*(1), 93–100.

Kumar, N. S., & Babu, K. C. (2021). A review on perovskite solar cells (PSCs), materials and applications. *Journal of Materiomics*, *7*.

Kumar, S., Vats, T., Sharma, S. N., & Kumar, J. (2018). Investigation of annealing effects on TiO2 nanotubes synthesized by a hydrothermal method for hybrid solar cells. *Optik - International Journal for Light and Electron Optics*. https://doi.org/10.1016/j.ijleo.2018.06.045

Lira-cantu, M., & Krebs, F. C. (2006). Hybrid solar cells based on MEH-PPV and thin film semiconductor oxides (TiO 2 , Nb 2 O 5 , ZnO , CeO 2 and CeO 2 – TiO 2): Performance improvement during long-time irradiation. *Solar Energy Materials & Solar Cells*, *90*, 2076–2086. https://doi.org/10.1016/j.solmat.2006.02.007

Liu, Y., Sun, J., Yang, Z., Yang, D., Ren, X., Xu, H., Yang, Z., & Liu, S. F. (2016). 20-mm-Large Single-Crystalline Formamidinium-Perovskite Wafer for Mass Production of Integrated Photodetectors. *Advanced Optical Materials*, *4*(11), 1829–1837. https://doi.org/10.1002/adom.201600327

Mahmood, K., Sarwar, S., & Mehran, M. T. (2017). Current status of electron transport layers in perovskite solar cells: materials and properties. *RSC Adv.*, *7*(28), 17044–17062. https://doi.org/10.1039/C7RA00002B

Moore, K., & Wei, W. (2021). Nano Materials Science Applications of carbon nanomaterials in perovskite solar cells for solar energy conversion. *Nano Materials Science*, *March*. https://doi.org/10.1016/j.nanoms.2021.03.005

Mosharraf Hossain Bhuiyan, M., Kabir, F., Serajum Manir, M., Saifur Rahaman, M., Barua, P., Ghosh, B., Mitsugi, F., & Ikegami, T. (2021). Improvement of Efficiency of Dye Sensitized Solar Cells by Incorporating Carbon Nanotubes. *Solar Cells [Working Title]*, 1–27. https://doi.org/10.5772/intechopen.96630

Nanoparticles, T., Al-bati, S., Hafizuddin, M., Jumali, H., Al-asbahi, B. A., & Farooq, W. A. (2020). Improving Photophysical Properties of White Emitting Ternary Conjugated Polymer Blend Thin. *Journal of Polymers*, *12*, 1–13.

Norhisamudin, N. A., Sabani, N., Rosli, N., Ahmad, M. F., Juhari, N., Shaari, S., & Zakaria, N. (2020). The efficiency effect of dye sensitized solar cell using different ratio of organic polymer doped titanium dioxide at different annealing process temperature. *AIP Conference Proceedings*, *2203*. https://doi.org/10.1063/1.5142144

Oyelade, O. V., Oyewole, O. K., Oyewole, D. O., Adeniji, S. A., Ichwani, R., Sanni, D. M., & Soboyejo, W. O. (2020). Pressure-Assisted Fabrication of Perovskite Solar Cells. *Scientific Reports*, *10*(1), 1–11. https://doi.org/10.1038/s41598-020-64090-5

Petrella, A, Tamborra, M., Cozzoli, P. D., Curri, M. L., Striccoli, M., Cosma, P., & Farinola, G. M. (2004). TiO 2 nanocrystals – MEH-PPV composite thin films as photoactive material. *Thin Solid Films*, *452*, 64–68. https://doi.org/10.1016/j.tsf.2003.10.106

Petrella, Andrea, Tamborra, M., Curri, M. L., Cosma, P., Striccoli, M., Cozzoli, P. D., Agostiano, A., Chimica, D., Uni, V., Orabona, V., Bari, I.-, Ipcf, C. N. R., Bari, S., Orabona, V., & Bari, I.-. (2005). Colloidal TiO 2 Nanocrystals / MEH-PPV Nanocomposites : Photo (electro) chemical Study. *J. Phys. Chem.*, *109*(4), 1554–1562.

Roy, P., Kumar, N., Tiwari, S., & Khare, A. (2020). A review on perovskite solar cells : Evolution of architecture , fabrication techniques , commercialization issues and status. *Solar Energy*, *198*(January), 665–688. https://doi.org/10.1016/j.solener.2020.01.080

Sarah, M. S. P., Zahid, F. S., Musa, M. Z., Noor, U. M., Shaameri, Z., Hamzah, A. S., & Rusop, M. (2011). Photoconductivity of Nanocomposite MEH-PPV : TiO 2 Thin Films. *Journal of Nano Research*, *13*, 87–92. https://doi.org/10.4028/www.scientific.net/JNanoR.13.87

Tripathi, D. C., Sinha, D. K., Suman, C. K., & Mohapatra, Y. N. (2006). Electrical characterization of solution processed MEHPPV/CNPPV hetrostructures. *Proc. of ASID*, 219–222.

Victoria, M., Haegel, N., Peters, I. M., Sinton, R., Ja, A., Can, C., Breyer, C., Stocks, M., Blakers, A., & Kaizuka, I. (2021a). *Perspective Solar photovoltaics is ready to power a sustainable future*. 1041–1056. https://doi.org/10.1016/j.joule.2021.03.005

Victoria, M., Haegel, N., Peters, I. M., Sinton, R., Ja, A., Can, C., Breyer, C., Stocks, M., Blakers, A., & Kaizuka, I. (2021b). Perspective Solar photovoltaics is ready to power a sustainable future. *Joule*, *5*, 1041–1056. https://doi.org/10.1016/j.joule.2021.03.005

Yang, L., Barrows, A. T., Lidzey, D. G., & Wang, T. (2016). Recent progress and challenges of organometal halide perovskite solar cells. *Reports on Progress in Physics*, *79*(2), 026501. https://doi.org/10.1088/0034-4885/79/2/026501

Yang, S. H., Le Rendu, P., Nguyen, T. P., & Hsu, C. S. (2007). Fabrication of MEH-PPV/SiO2 and MEH-PPV/TiO2 nanocomposites with enhanced luminescent stabilities. *Reviews on Advanced Materials Science*, *15*(2), 144–149.

Zahid, F. S. ., Sarah, M. S. ., & Rusop, M. (2012). The effect of TiO2 Nanoparticle on the Photoconductivity Properties of Organic MEH-PPV Thin Films for Organic Photovoltaic Cell Applications. *Humanities, Science and Engineering Research ?MJ*, *0*, 513–517.

Zheng, L., Zhang, D., Ma, Y., Lu, Z., Chen, Z., Wang, S., Xiao, L., & Gong, Q. (2015). Morphology control of the perovskite films for efficient solar cells. *Dalton Trans.*, *44*(23), 10582–10593. https://doi.org/10.1039/C4DT03869J